

Experimental Physics 3 Course on Optics and Quantum Mechanics

Frank Cichos

2024-10-20

Table of contents

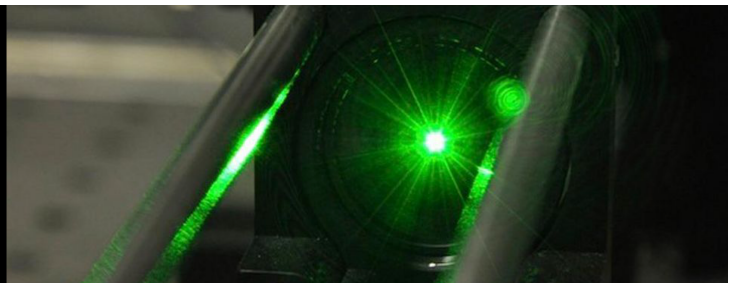
1 Experimental Physics	3	1
2 Welcome to the Experimental Physics 3 Course!		3
I Geometrical Optics		5
3 Geometrical Optics		7
3.1 Learning Objectives		7
3.2 Topics Covered		7
3.3 Introduction		7
3.4 Assumptions of Geometrical Optics		7
4 Reflection		9
4.0.1 Law of Reflection		9
4.0.2 Fermat's Principle		10
4.0.3 Action Integral		11
4.0.4 Lagrangian		11
4.0.5 Euler-Lagrange Equations		12
4.0.6 Example: Simple Harmonic Oscillator		12
5 Refraction and Total Internal Reflection		13
5.1 Refraction		13
5.1.1 Refractive Index		14
5.1.2 Snells Law		14
5.1.3 Total Internal Reflection		15
5.1.4 Fermat's Principle for Inhomogeneous Media		18
6 Optical Elements Part I		25
6.1 Mirrors		25
6.1.1 Plane Mirrors		25
6.1.2 Concave Mirrors		26
7 Optical Elements Part II		35
7.1 Prism		35
7.1.1 Deflection angle		35
7.1.2 Minimum deflection angle		36
7.1.3 Dispersion		37
7.1.4 Prims spectrograph		39
8 Optical Elements Part III		43
8.0.1 Lenses		43
8.0.2 Thin lens		46
8.0.3 Thick lens		49

8.1	Derivation	51
8.1.1	Lens types	52
9	Optical Instruments	55
9.1	The Human Eye	55
9.1.1	Key Components and Their Functions	55
9.1.2	Optical Properties of the Eye	56
9.1.3	Photoreceptors: Cones and Rods	56
9.1.4	Visual Acuity and Performance	56
9.1.5	Resolution Limit of the Eye	57
9.1.6	Refractive Errors and Visual Correction	57
9.1.7	Magnification	58
10	Optical Instruments	61
10.1	Magnifying Glass	61
11	Optical Instruments	63
11.1	Microscope	63
11.1.1	Confocal Microscopy	67
11.1.2	Examples for Super-Resolution Microscopy Techniques	68

Chapter 1

Experimental Physics 3

Experimental
Physics 3



Chapter 2

Welcome to the Experimental Physics 3 Course!

In this Experimental Physics 3 course, we will explore fundamental experiments and mathematical descriptions related to light propagation, electromagnetic waves, and their material counterpart, matter waves. Specifically, we will focus on:

- Geometrical Optics
- Wave Optics
- Electromagnetic Waves
- Matter Waves and Quantum Mechanics

The fields of optics and quantum mechanics are currently vibrant areas of research, with rapidly evolving optical technologies, high-resolution microscopy, and quantum information science. All of these advancements build upon the foundations that we will address in this course.

Part I

Geometrical Optics

Chapter 3

Geometrical Optics

In this section, we will explore the fundamental principles that govern how light behaves when it encounters different media and surfaces.

3.1 Learning Objectives

By the end of this section, you should be able to:

- Understand and apply the laws of reflection and refraction.
- Analyze image formation by mirrors, lenses, and prisms.
- Describe the working principles of various optical instruments.
- Explain phenomena such as dispersion and imaging errors.

3.2 Topics Covered

1. **Reflection** Explore how light reflects off surfaces following the law of reflection.
2. **Refraction and Total Internal Reflection** Understand how light bends when passing through different media and the conditions for total internal reflection.
3. **Mirrors, Prisms and Lenses** Learn about various optical elements and how they form images.
4. **Optical Instruments** Study devices like telescopes and microscopes that utilize mirrors and lenses.
5. **Dispersion** Discover how different wavelengths of light refract differently, leading to phenomena like rainbows.
6. **Imaging Errors** Examine common aberrations in optical systems and methods to correct them.

3.3 Introduction

Geometrical optics is an approximate description of light propagation in the limit of infinitely small wavelength, where all wave phenomena like diffraction can be neglected.

Light interacts with materials in predictable ways, allowing us to design optical systems for imaging, magnification, and more.

3.4 Assumptions of Geometrical Optics

Geometrical optics provides an approximate description of light behavior and is based on several key assumptions. These assumptions simplify the complex nature of light while still allowing for accurate predictions in many practical scenarios.

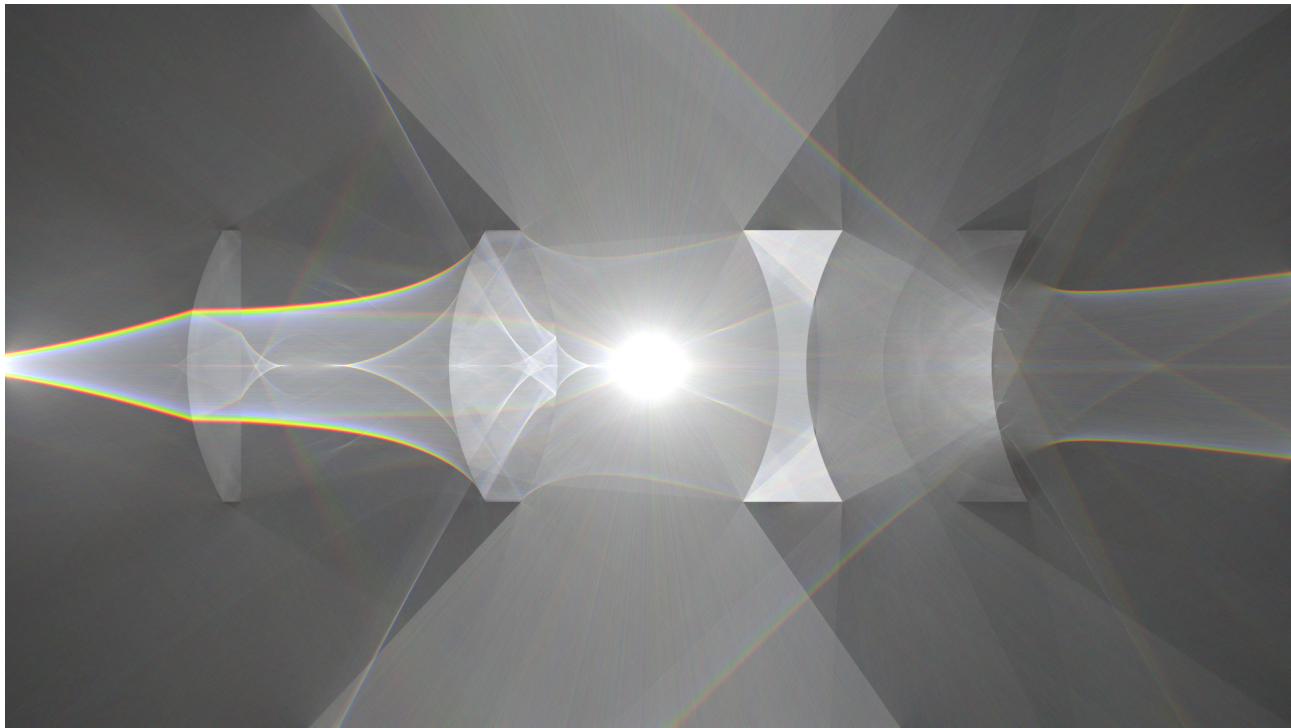


Figure 3.1: Light rays passing through a lens system generated with [Tantalum](#)

i Core Assumptions

1. Light Sources and Detection:

- Light rays emerge from a light source
- Light rays are detected by a detector

2. Light-Matter Interaction:

- Interaction is characterized by a refractive index n
- The speed of light in a medium is given by $c = c_0/n$, where c_0 is the speed of light in vacuum
- The speed in vacuum is **299.792.458 m/s** and is connected to the definition of the meter

3. Light Propagation:

- Light propagates in straight line paths (rays) in a homogeneous medium
- Light bends to a curved path in inhomogeneous media with varying refractive index $n(\mathbf{r})$

4. Behavior at Interfaces:

- Rays may be reflected and refracted at interfaces between media

These assumptions form the foundation for understanding and predicting light behavior in the context of geometrical optics.

Chapter 4

Reflection

Historical Context of Reflection Laws

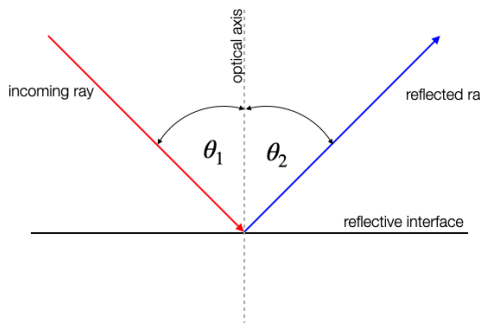
The study of reflection has a rich history dating back to ancient times:

1. **Ancient Greece (300 BCE)**: Euclid, in his work “Catoptrics,” was among the first to formally describe the law of reflection. He stated that the angle of incidence equals the angle of reflection.
2. **Ancient Rome (50 CE)**: Hero of Alexandria expanded on Euclid’s work, applying the principle that light travels along the path of least distance.
3. **Islamic Golden Age (1000 CE)**: Ibn al-Haytham (Alhazen) made significant contributions to optics in his “Book of Optics.” He conducted experiments to verify the law of reflection and explored the properties of spherical and parabolic mirrors.
4. **17th Century**: Fermat’s Principle, formulated by Pierre de Fermat, provided a more general framework for understanding reflection (and refraction) based on the principle of least time.
5. **Modern Era**: The understanding of reflection has been further refined with the development of electromagnetic theory by James Clerk Maxwell in the 19th century and quantum optics in the 20th century.

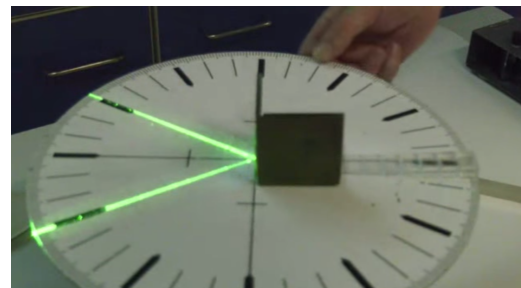
The law of reflection is probably the most simple one. Yet the simplicity gives us the chance to define some basic objects which we will further use for the description of light rays and their propagation.

4.0.1 Law of Reflection

The sketch below shows the reflection of an incoming light ray (red) on an interface. This incoming light ray has an angle θ_1 with the axis (dashed line), which is perpendicular to the reflecting surface. As compared to X-ray diffraction, we measure the angle to the normal of the surface and not to the surface itself.



(a) Law of reflection



(b) Experimental Demonstration

Figure 4.1: Figure 4.1a illustrates the law of reflection, while Figure 4.1b shows an experimental demonstration.

Figure 4.1a shows the reflection of an incoming light ray (red) on an interface. This incoming light ray has an angle θ_1 with the axis (dashed line), which is perpendicular to the reflecting surface. As compared to X-ray diffraction, we measure the angle to the normal of the surface and not to the surface itself.

The law of reflection tells us now, that the outgoing reflected ray is now leaving the surface under an angle $\theta_2 = \theta_1$. So both angles are the same for the reflection.

Law of Reflection

If a ray is incident to a reflecting surface under an angle θ_1 it will be reflected towards under an angle $\theta_2 = \theta_1$ to the same side of the surface.

4.0.2 Fermat's Principle

The law of reflection can be actually obtained from a variational principle saying the light rays propagate along those path on which the propagation time is an extremum. This variational principle is called Fermat's principle.

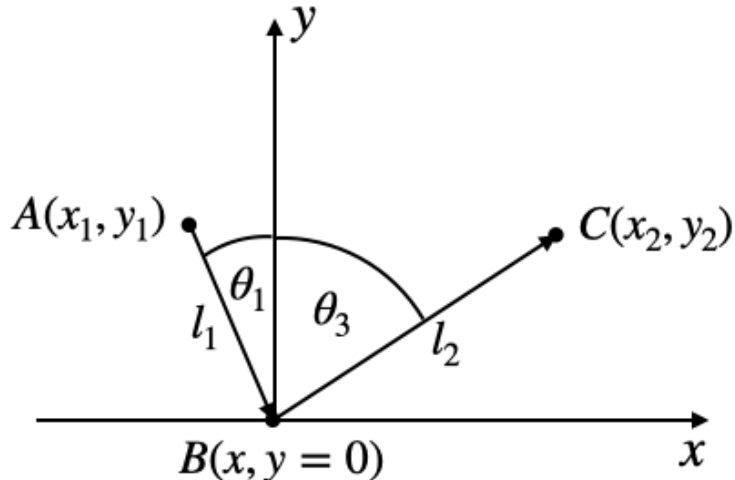


Figure 4.2: Sketch for deriving the law of reflection from Fermat's principle

Consider now a light ray that should travel from point A to point C via a point B on the mirror surface. In general multiple paths are possible such as the one indicated in the above picture. Clearly this path is not satisfying our reflection law formulated above. Fermat's principle now restricts the path length from A to C to be the one, which takes the least amount of time.

Fermat's principle

The path taken by a ray between two given points A, B is the path that can be traversed in the least time.

More precise alternative: A ray going in a certain particular path has the property that if we make a small change in the ray in any manner whatever, say in the location at which it comes to the mirror, or the shape of the curve, or anything, there will be no first-order change in the time; there will be only a second-order change in the time.

So let us consider that constraints to the path length. The total length the light hast to travel via the three points is

$$l = l_1 + l_2 = \sqrt{(x - x_1)^2 + y_1^2} + \sqrt{(x_2 - x)^2 + y_2^2}$$

The time that is required by the light to travel that distance l is then given by

$$t = \frac{l}{c},$$

where c is the speed of light in the medium above the mirror. If this time should now be a minimum, we have to take the derivative of the time t with respect to the position x on the mirror and set that to zero, i.e.,

$$\frac{dt}{dx} = 0. \quad (4.1)$$

This results in Equation 4.1

$$\frac{x - x_1}{\sqrt{(x - x_1)^2 + y_1^2}} = \frac{x_2 - x}{\sqrt{(x_2 - x)^2 + y_2^2}},$$

which is actually

$$\frac{x - x_1}{l_1} = \frac{x_2 - x}{l_2}$$

or

$$\sin(\theta_1) = \sin(\theta_2)$$

which finally requires

$$\theta_1 = \theta_2$$

and is our law of reflection. Thus, reflection satisfies Fermat's principle, i.e. the light rays propagate along those path on which the propagation time is an extremum.

💡 Principle of Least Action (Hamilton's Principle)

The Principle of Least Action, also known as Hamilton's Principle, is a fundamental concept in classical mechanics. It states that the path taken by a physical system between two states is the one for which the action integral is stationary (usually a minimum).

4.0.3 Action Integral

The action S is defined as the integral of the Lagrangian L over time:

$$S = \int_{t_1}^{t_2} L dt$$

4.0.4 Lagrangian

The Lagrangian L is a function that summarizes the dynamics of the system. For a system with generalized coordinates q_i and velocities \dot{q}_i , the Lagrangian is typically given by:

$$L = T - V$$

where:

- T is the kinetic energy of the system.
- V is the potential energy of the system.

4.0.5 Euler-Lagrange Equations

Hamilton's Principle leads to the Euler-Lagrange equations, which are the equations of motion for the system. These equations are derived by requiring that the action S be stationary with respect to variations in the path $q_i(t)$:

$$\delta S = 0$$

This condition leads to the following differential equations:

$$\frac{d}{dt} \left(\frac{\partial L}{\partial \dot{q}_i} \right) - \frac{\partial L}{\partial q_i} = 0$$

These are the Euler-Lagrange equations, and they provide a powerful method for deriving the equations of motion for a wide variety of physical systems.

4.0.6 Example: Simple Harmonic Oscillator

For a simple harmonic oscillator with mass m and spring constant k , the Lagrangian is:

$$L = \frac{1}{2}m\dot{x}^2 - \frac{1}{2}kx^2$$

Applying the Euler-Lagrange equation:

$$\frac{d}{dt} \left(\frac{\partial L}{\partial \dot{x}} \right) - \frac{\partial L}{\partial x} = 0$$

we get:

$$m\ddot{x} + kx = 0$$

which is the familiar equation of motion for a simple harmonic oscillator.

Hamilton's Principle and the associated Euler-Lagrange equations are foundational in classical mechanics and have far-reaching implications in other areas of physics, including quantum mechanics and field theory.

Chapter 5

Refraction and Total Internal Reflection

5.1 Refraction

Historical Context of Refraction

The understanding of refraction has evolved over centuries, with contributions from various cultures and scientific traditions. This timeline highlights key milestones in the discovery and formalization of refraction, showcasing how our comprehension of this fundamental optical phenomenon has deepened over time:

1. **Ancient Greece (3rd century BCE):** Euclid noticed that a stick partially submerged in water appears bent. Archimedes studied the refraction of light in water.
2. **Ancient Rome (1st century CE):** Ptolemy conducted experiments on refraction and compiled tables of refraction angles for different media.
3. **Islamic Golden Age (10th-11th centuries):** Ibn Sahl (940-1000) discovered the law of refraction, describing it geometrically. Alhazen (965-1040) studied lenses and the human eye, contributing significantly to optics.
4. **Middle Ages:** Robert Grosseteste (1175-1253) and Roger Bacon (1214-1294) studied refraction and its application to lenses.
5. **Renaissance:** Thomas Harriot (1560-1621) rediscovered the law of refraction but didn't publish his findings.
6. **17th Century:** Willebrord Snellius (1580-1626) derived the mathematical law of refraction (Snell's law) around 1621. René Descartes (1596-1650) independently derived and published the law of refraction in 1637. Pierre de Fermat (1607-1665) derived the law of refraction using his principle of least time.
7. **19th Century:** Augustin-Jean Fresnel (1788-1827) developed the wave theory of light, explaining refraction in terms of changes in wave speed.
8. **20th Century:** The quantum mechanical understanding of light, which emerged in the early 20th century, significantly impacted our view of refraction. Max Planck's work on black body radiation in 1900 and Albert Einstein's explanation of the photoelectric effect in 1905 laid the groundwork for the quantum nature of light. This quantum perspective provided a complementary explanation to the wave theory, describing refraction in terms of photons interacting with the atoms in the medium. While this quantum view offers insights into certain aspects of refraction, it's important to note that both the wave and particle descriptions of light are necessary for a complete understanding of optical phenomena.

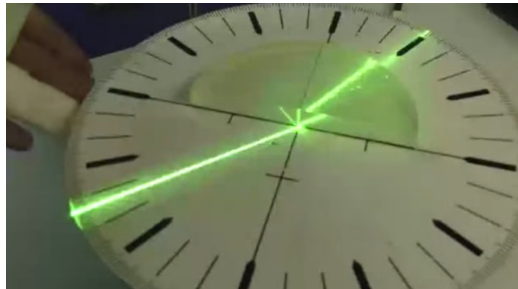
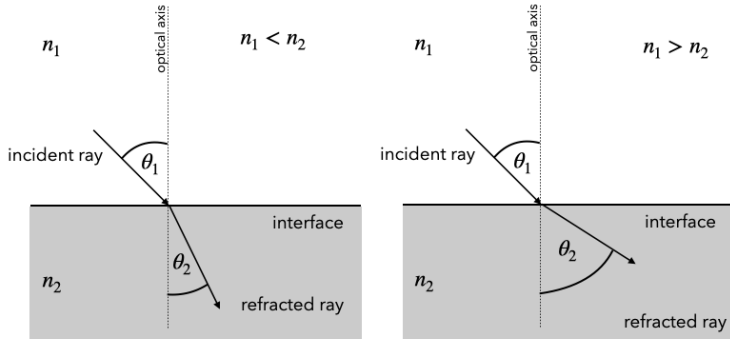
The law of refraction is the second important law of geometrical optics. It relates the refractive index n_1 and angle of incidence θ_1 on one side of an interface to the refractive index n_2 and angle of refraction θ_2 on the other side. Both the law of reflection and the law of refraction can be derived from more fundamental principles

such as Fermat's principle of least time and are consistent with the conservation of energy. Their relation to momentum is more complex and involves considering the interaction of light with the medium at an atomic level. These laws provide a mathematical framework for predicting how light behaves when it encounters interfaces between different media, forming the basis for understanding a wide range of optical phenomena and the design of optical devices.

5.1.1 Refractive Index

The refractive index n is a material constant representing the factor by which the speed of light is reduced in the medium compared to its speed in vacuum. For most natural materials and visible light, the refractive index is $n \geq 1$, as light typically travels slower in media than in vacuum. However, in certain special cases—such as for X-rays in some materials or in engineered metamaterials—the refractive index can be less than 1 or even negative. Understanding these exotic cases requires a deeper exploration of the electromagnetic properties of materials and the origin of the refractive index, which we will address later.

5.1.2 Snells Law



Law of Refraction (Snell's Law)

The law of refraction (Snell's law) is given for the above sketch by the equation:

$$n_1 \sin(\theta_1) = n_2 \sin(\theta_2)$$

You can explore the law of refraction using the interactive visualization below. The visualization shows a light ray incident on an interface between two media with different refractive indices. You can adjust the angle of incidence and the refractive index of the first medium to see how the angle of refraction changes according to Snell's law.

Snell's law leads to some general patterns in the behavior of light rays at interfaces, which are worth remembering. Consider these two cases:

1. When light moves from a medium with lower refractive index to one with higher refractive index ($n_1 < n_2$):
 - The refracted ray bends towards the normal (optical axis)
 - The angle of refraction is smaller than the angle of incidence ($\theta_2 < \theta_1$)
2. When light moves from a medium with higher refractive index to one with lower refractive index ($n_1 > n_2$):

- The refracted ray bends away from the normal (optical axis)
- The angle of refraction is larger than the angle of incidence ($\theta_2 > \theta_1$)

Figure 5.1 illustrates these principles with three plots showing how the refracted angle changes with the incident angle for two common interface scenarios: glass-to-air and air-to-glass. These plots clearly demonstrate the different behaviors described above.

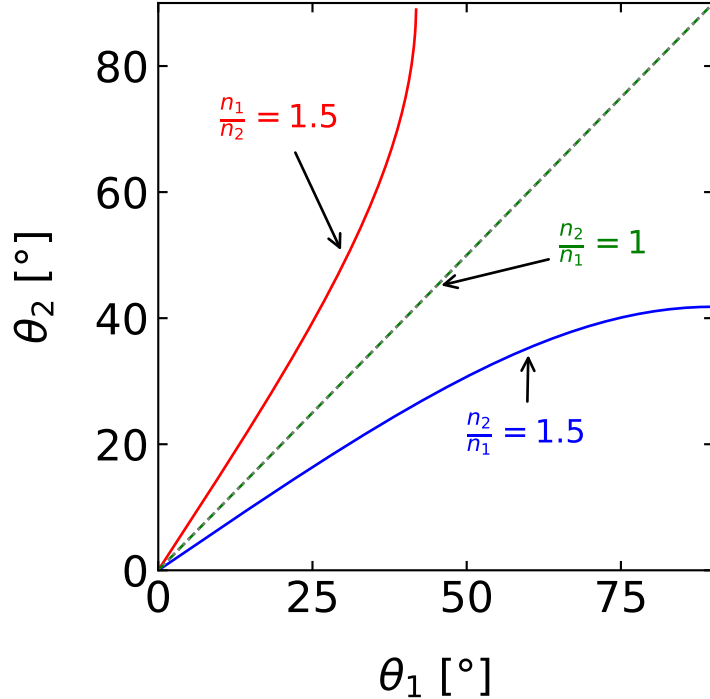


Figure 5.1: Snell's law for different combinations of refractive indices. The plots show the relationship between incident angle (θ_1) and refracted angle (θ_2) for three scenarios: (a) light passing from air to glass, (b) light passing from glass to air, and (c) a comparison of both cases. Note how the curves differ when light moves into a medium with higher refractive index versus a lower refractive index.

5.1.3 Total Internal Reflection

The above diagram reveals a special case occurring when $n_1 > n_2$. Under these conditions, we can increase the incident angle θ_1 until the outgoing angle reaches $\theta_2 = \frac{\pi}{2}$. At this point, the refracted ray would be traveling along the interface between the two media. For any incident angle θ_1 larger than this critical angle, there is no refracted ray at all; instead, we observe only a reflected ray. This phenomenon, known as **total internal reflection**, occurs despite the fact that the material with refractive index n_2 is completely transparent.

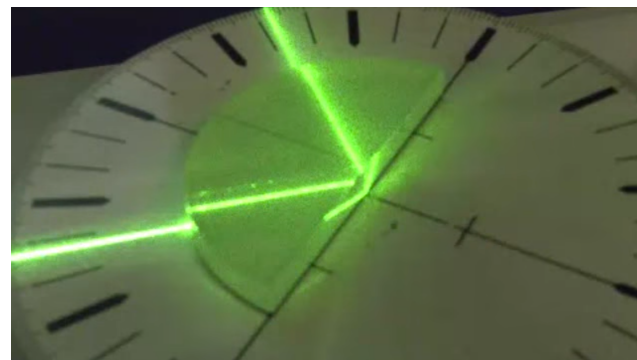
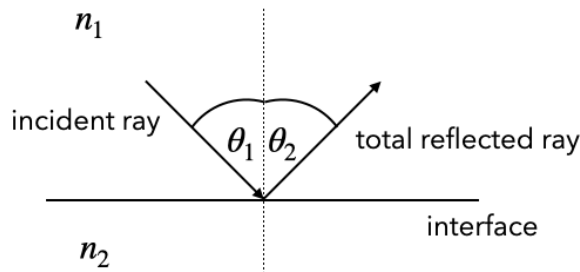
Let's formalize this concept mathematically. Using Snell's law and setting $\theta_2 = \frac{\pi}{2}$, we obtain the equation for the critical angle θ_c :

$$\theta_1 = \theta_c = \sin^{-1} \left(\frac{n_2}{n_1} \right)$$

Note that the $\sin^{-1}()$ function requires an argument ≤ 1 , which is why this phenomenon only occurs when $n_2 < n_1$.

It's important to understand that during total internal reflection, all of the light energy is reflected back into the first medium, hence the term 'total'. However, electromagnetic optics reveals an interesting subtlety: an evanescent wave penetrates a short distance into the second medium, though it doesn't propagate energy across the boundary.

When the incident angle exceeds the critical angle, Snell's law as we've written it no longer applies. Instead, we observe perfect reflection, where the angle of reflection equals the angle of incidence, just as in regular reflection from a mirror. This reflection occurs without any loss of energy to the second medium, making it an extremely efficient process.

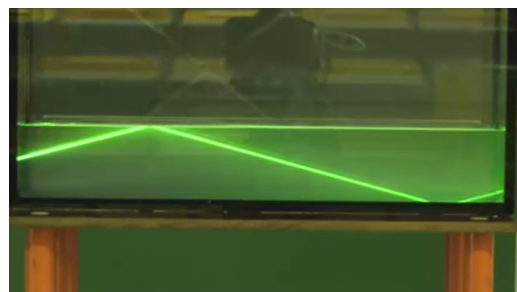
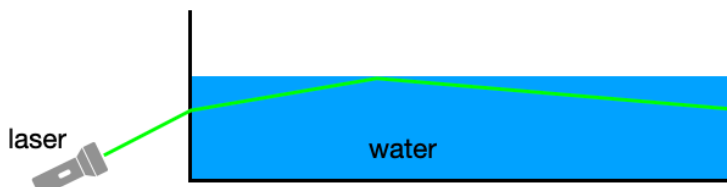


Total Internal Reflection

Total internal reflection occurs when light is passing from higher refractive index to lower refractive index materials for incidence angle larger than a critical angle

$$\theta_c = \sin^{-1} \left(\frac{n_2}{n_1} \right)$$

We can demonstrate total internal reflection very easily with a water basin, for example, where we couple in light from a laser from the side.



But you could try that yourself also in the bath tub diving below the water surface.

Total internal reflection has numerous practical applications:

1. Fiber optic communications: Light signals can travel long distances with minimal loss through optical fibers.
2. Optical instruments: Prisms in binoculars and telescopes use total internal reflection to manipulate light paths.
3. Gemstones: The sparkle of diamonds is enhanced by total internal reflection trapping light within the stone.
4. Medical endoscopes: Total internal reflection helps guide light through flexible tubes for internal imaging.

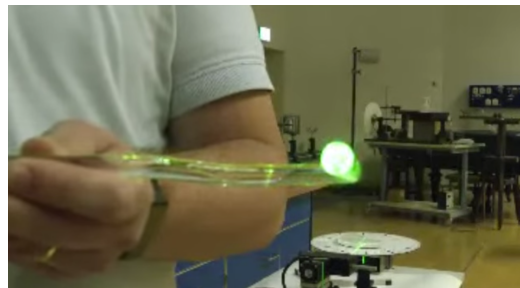
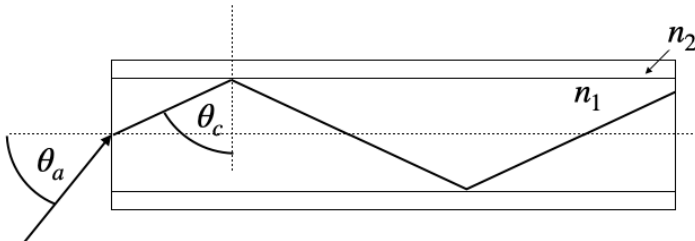
Optical Fibers and Total Internal Reflection

Total internal reflection plays a crucial role in modern telecommunications, particularly in optical fibers, which are also part of many experimental setups. These fibers are essentially ultra-thin glass wires, ranging in diameter from a few micrometers to several hundred micrometers, designed to transport light over long distances with minimal loss.

The structure of an optical fiber is key to its function:

1. Core: A central glass core with a refractive index n_1
2. Cladding: A surrounding layer with a slightly lower refractive index n_2

This difference in refractive indices is what allows total internal reflection to occur within the fiber.



For light to propagate effectively through the fiber, it must enter at an angle that ensures total internal reflection at the core-cladding interface. This leads to the concept of the acceptance angle, θ_a , which is the maximum angle at which light can enter the fiber and still undergo total internal reflection.

To characterize this acceptance angle, optical engineers use a parameter called the **Numerical Aperture (NA)**.

Numerical Aperture

The Numerical Aperture of a fiber is defined as the sine of the maximum acceptance angle:

$$NA = \sin(\theta_a) = \sqrt{n_1^2 - n_2^2} \quad (5.1)$$

This equation relates the NA directly to the refractive indices of the core and cladding. The derivation of this formula involves applying Snell's law at the air-fiber interface and at the core-cladding interface, then using the

condition for total internal reflection.

In practice, typical values for the refractive indices might be $n_1 = 1.475$ for the core and $n_2 = 1.46$ for the cladding. Plugging these into our equation:

$$NA = \sqrt{1.475^2 - 1.46^2} \approx 0.2 \quad (5.2)$$

This means that light entering the fiber within a cone of about 11.5° ($\arcsin(0.2)$) from the fiber's axis will be transmitted through the fiber via total internal reflection.

The NA is an important parameter in fiber optic design:

1. It determines the light-gathering ability of the fiber.
2. It affects the fiber's bandwidth and its susceptibility to certain types of signal distortion.
3. It influences how easily the fiber can be coupled to light sources and other fibers.

Optical fibers come in various types, each optimized for different applications. Some fibers are designed to transmit light over long distances with minimal loss, while others are engineered for specific wavelengths or to guide light in unusual ways. The figure below shows a few examples of optical fiber types.

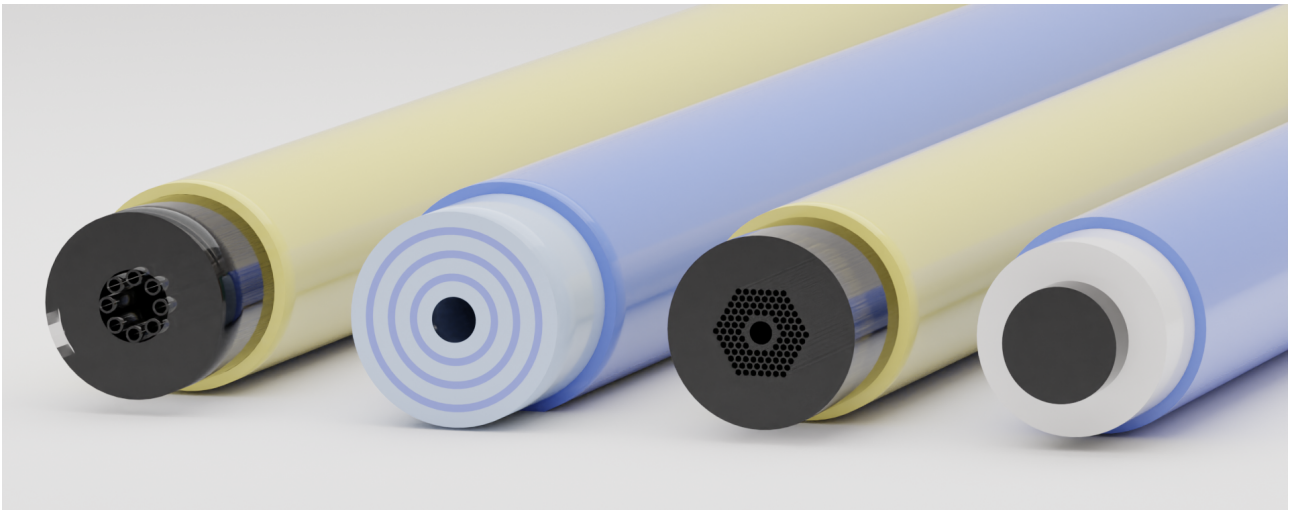


Figure 5.2: Rendering of different optical fibers types (from left to right): Hollow core optical fiber, hollow core bragg fiber, photonic crystal fiber, conventional fiber

5.1.4 Fermat's Principle for Inhomogeneous Media

While before we have considered Fermat's principle for the special case of refraction and light propagation in a homogeneous medium, we can define a more general version of it corresponding to the following situation also involving an inhomogeneous refractive index $n(\vec{r})$.

For this general scenario of light traveling along a path, we can define an optical path length (OPL) as

$$\text{OPL} = \int_A^C n(\mathbf{r}) ds = 0, \quad (5.3)$$

with a varying refractive index $n(\mathbf{r})$. Fermat's Principle states that the actual path taken by the light makes the OPL stationary:

$$\delta \left(\int_A^B n(\mathbf{r}) ds \right) = 0$$

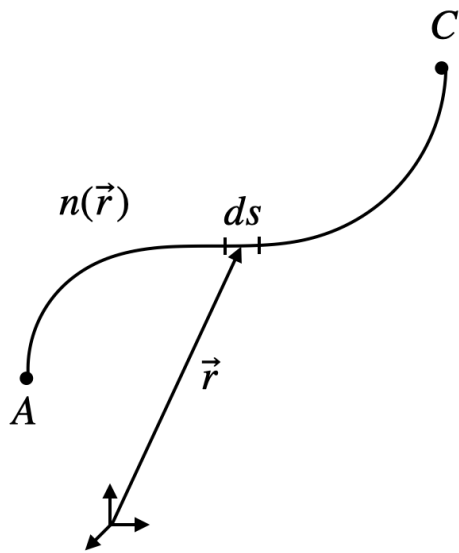


Figure 5.3: Sketch for a general description of Fermat's principle

Using the calculus of variations, this leads to the Euler-Lagrange equation for the path of light. In Cartesian coordinates, if the path is parameterized by $\mathbf{r}(s) = (x(s), y(s), z(s))$, the Euler-Lagrange equations become:

$$\frac{d}{ds} \left(n \frac{d\mathbf{r}}{ds} \right) = \nabla n$$

where ∇n is the gradient of the refractive index. This equation describes how the light ray bends in response to changes in the refractive index of the medium.

Fermat's Principle is a cornerstone of geometrical optics and has applications in designing optical systems, understanding mirages, and analyzing the behavior of light in various media.

Fermat's Principle and Snells Law

We would like to apply Fermat's principle to derive Snell's law, which is a more lengthy calculation. To do this, we consider a light ray traveling from point A in medium 1 (with refractive index n_1) to point C in medium 2 (with refractive index n_2), crossing the interface at point B . Let the coordinates of points A , B , and C be (x_A, y_A) , (x_B, y_B) , and (x_C, y_C) , respectively. Assume the interface between the two media is at $y = y_B$. The optical path length (OPL) is given by:

$$\delta \int_A^C n(\vec{r}) ds = 0,$$

where $n(\vec{r})$ is the refractive index at position \vec{r} , and ds is an infinitesimal element of the path.

Consider a light ray traveling from point A in medium 1 (with refractive index n_1) to point C in medium 2 (with refractive index n_2), crossing the interface at point B . Let the coordinates of points A , B , and C be (x_A, y_A) , (x_B, y_B) , and (x_C, y_C) , respectively. Assume the interface between the two media is at $y = y_B$.

Optical Path Length

The optical path length (OPL) is given by:

$$\text{OPL} = n_1 \int_A^B ds_1 + n_2 \int_B^C ds_2,$$

where ds_1 and ds_2 are the infinitesimal path lengths in media 1 and 2, respectively.

Path Lengths

The path lengths ds_1 and ds_2 can be expressed in terms of the coordinates:

$$ds_1 = \sqrt{(dx_1)^2 + (dy_1)^2}, \quad ds_2 = \sqrt{(dx_2)^2 + (dy_2)^2}.$$

Since the interface is at $y = y_B$, we have $dy_1 = y_B - y_A$ and $dy_2 = y_C - y_B$. The total optical path length is:

$$\text{OPL} = n_1 \sqrt{(x_B - x_A)^2 + (y_B - y_A)^2} + n_2 \sqrt{(x_C - x_B)^2 + (y_C - y_B)^2}.$$

Applying Fermat's Principle

To find the stationary path, we take the variation of the OPL with respect to x_B :

$$\delta \text{OPL} = \delta \left[n_1 \sqrt{(x_B - x_A)^2 + (y_B - y_A)^2} + n_2 \sqrt{(x_C - x_B)^2 + (y_C - y_B)^2} \right] = 0.$$

Taking the derivative with respect to x_B :

$$\frac{\partial}{\partial x_B} \left[n_1 \sqrt{(x_B - x_A)^2 + (y_B - y_A)^2} + n_2 \sqrt{(x_C - x_B)^2 + (y_C - y_B)^2} \right] = 0.$$

Differentiating

Differentiating each term separately:

$$n_1 \frac{\partial}{\partial x_B} \sqrt{(x_B - x_A)^2 + (y_B - y_A)^2} + n_2 \frac{\partial}{\partial x_B} \sqrt{(x_C - x_B)^2 + (y_C - y_B)^2} = 0.$$

Using the chain rule:

$$n_1 \frac{x_B - x_A}{\sqrt{(x_B - x_A)^2 + (y_B - y_A)^2}} + n_2 \frac{x_B - x_C}{\sqrt{(x_C - x_B)^2 + (y_C - y_B)^2}} = 0.$$

Simplifying

Let θ_1 be the angle of incidence and θ_2 be the angle of refraction. Then:

$$\sin \theta_1 = \frac{x_B - x_A}{\sqrt{(x_B - x_A)^2 + (y_B - y_A)^2}}, \quad \sin \theta_2 = \frac{x_C - x_B}{\sqrt{(x_C - x_B)^2 + (y_C - y_B)^2}}.$$

Substituting these into the equation:

$$n_1 \sin \theta_1 + n_2 \sin \theta_2 = 0.$$

Since $\sin \theta_2$ is in the opposite direction, we have:

$$n_1 \sin \theta_1 = n_2 \sin \theta_2.$$

This is Snell's law, which describes the relationship between the angles of incidence and refraction when light passes from one medium to another.

Conclusion

By applying Fermat's principle and taking the variation of the optical path length, we have derived Snell's law:

$$n_1 \sin \theta_1 = n_2 \sin \theta_2.$$

This demonstrates how the principle of least time leads to the well-known law of refraction in optics.

 Example: Light in a Graded-Index Medium

Consider a medium where the refractive index varies with height y as $n(y) = n_0(1 - \frac{\alpha^2}{2n_0}y^2)$. The path of light in such a medium can be found by using Fermat's principle in differential form:

$$\frac{d}{ds} \left(n(\mathbf{r}) \frac{d\mathbf{r}}{ds} \right) = \nabla n(\mathbf{r})$$

Typically, this requires to express the coordinates in terms of a parameter, such as $x(s)$ and $y(s)$, and then solve the differential equation. The solution will give the path of light in the medium. This is difficult and commonly done numerically. In paraxial optics, when the light is propagating roughly in the direction of z , the differential element ds can be approximated as dz since then

$$ds = dz \sqrt{1 + \left(\frac{dy}{dz} \right)^2 + \left(\frac{dx}{dz} \right)^2} \approx dz$$

which yields

$$\frac{d}{dz} \left(n \frac{dx}{dz} \right) \approx \frac{dn}{dx}$$

and

$$\frac{d}{dz} \left(n \frac{dy}{dz} \right) \approx \frac{dn}{dy}$$

This readily yields the path of light in a homogeneous medium, where n is constant. In this case we have

$$\frac{d^2x}{dz^2} = \frac{d^2y}{dz^2} = 0$$

which is true for a straight line. In a graded-index medium, the path of light can be found by solving the differential equation

$$\frac{d^2y}{dz^2} = -\alpha^2 y$$

which is reminiscent of the equation of motion of a harmonic oscillator. The solution is therefore an oscillating function

$$y(z) = y_0 \cos(\alpha z) + \frac{\theta_0}{\alpha} \sin(\alpha z)$$

where the angle θ_0 is the initial angle of the light ray with respect to the z axis. This solution describes the path of light in a graded-index medium.

 Fermat's Principle in Integral and Differential Form

We have described Fermat's principle in an integral form specifying the optical path length S as

$$OPL = \int n(\mathbf{r}) ds$$

The path length ds can be given in terms of two coordinates x_1 and x_2 parametrized by λ such that

$$ds = \sqrt{\dot{x}_1^2 + \dot{x}_2^2} d\lambda$$

where $\dot{x}_1 = \frac{dx_1}{d\lambda}$. We can therefore write Fermat's principle as

$$\delta OPL = \int \left[\left(\frac{\partial n}{\partial x_i} \delta x_i \right) \sqrt{\dot{x}_1^2 + \dot{x}_2^2} + n \frac{1}{\sqrt{\dot{x}_1^2 + \dot{x}_2^2}} \dot{x}_i \delta \dot{x}_i \right] d\lambda = 0$$

To evaluate this integral we would like to integrate by parts. We can write the integrand as

$$u = n \frac{1}{\sqrt{\dot{x}_1^2 + \dot{x}_2^2}} \dot{x}_i$$

and

$$dv = \delta \dot{x}_i d\lambda$$

We can now calculate du and v and obtain

$$du = \frac{d}{d\lambda} \left[n \frac{1}{\sqrt{\dot{x}_1^2 + \dot{x}_2^2}} \dot{x}_i \right] d\lambda$$

and

$$v = \delta x_i$$

With these expressions we can now apply the integration by parts formula $\int u dv = uv - \int v du$, we get:

$$\int n \frac{1}{\sqrt{\dot{x}_1^2 + \dot{x}_2^2}} \dot{x}_i \delta \dot{x}_i d\lambda = \left[n \frac{1}{\sqrt{\dot{x}_1^2 + \dot{x}_2^2}} \dot{x}_i \delta x_i \right] \Big|_{\lambda_1}^{\lambda_2} - \int \delta x_i \frac{d}{d\lambda} \left[n \frac{1}{\sqrt{\dot{x}_1^2 + \dot{x}_2^2}} \dot{x}_i \right] d\lambda$$

This can be substituted back into the original equation to obtain

$$\begin{aligned} \delta OPL &= \int \left[\left(\frac{\partial n}{\partial x_i} \delta x_i \right) \sqrt{\dot{x}_1^2 + \dot{x}_2^2} \right] d\lambda \\ &\quad + \left[n \frac{1}{\sqrt{\dot{x}_1^2 + \dot{x}_2^2}} \dot{x}_i \delta x_i \right] \Big|_{\lambda_1}^{\lambda_2} \\ &\quad - \int \delta x_i \frac{d}{d\lambda} \left[n \frac{1}{\sqrt{\dot{x}_1^2 + \dot{x}_2^2}} \dot{x}_i \right] d\lambda = 0 \end{aligned}$$

After rearranging the terms we get

$$\begin{aligned} \delta OPL &= \int \left\{ \frac{\partial n}{\partial x_i} \sqrt{\dot{x}_1^2 + \dot{x}_2^2} - \frac{d}{d\lambda} \left[n \frac{1}{\sqrt{\dot{x}_1^2 + \dot{x}_2^2}} \dot{x}_i \right] \right\} \delta x_i d\lambda \\ &\quad + \left[n \frac{1}{\sqrt{\dot{x}_1^2 + \dot{x}_2^2}} \dot{x}_i \delta x_i \right] \Big|_{\lambda_1}^{\lambda_2} = 0 \end{aligned}$$

and therefore finally

$$\delta OPL = \int \left[\left(\frac{\partial n}{\partial x_i} \right) \sqrt{\dot{x}_1^2 + \dot{x}_2^2} - \frac{d}{d\lambda} \left(n \frac{1}{\sqrt{\dot{x}_1^2 + \dot{x}_2^2}} \dot{x}_i \right) \right] \delta x_i d\lambda + \text{boundary terms}$$

for which we choose the parameter λ such that the boundary terms vanish.

$$\lambda = s$$

such that

$$\sqrt{\dot{x}_1^2 + \dot{x}_2^2} = 1$$

and finally leads to the Euler-Lagrange equation

$$\left(\frac{\partial n}{\partial x_i} \right) - \frac{d}{ds} (n \dot{x}_i) = 0$$

which is the differential form of the Fermat's principle.

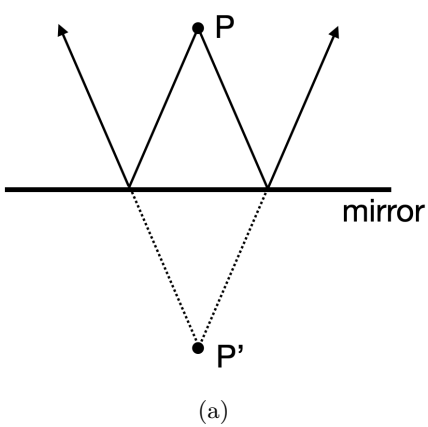
Chapter 6

Optical Elements Part I

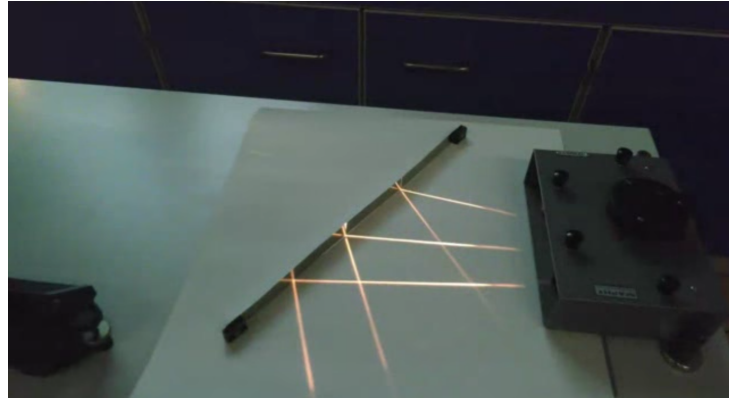
6.1 Mirrors

6.1.1 Plane Mirrors

When light radiates from a point P and reflects off a mirror, as shown in the image, the reflected rays diverge but appear to originate from a point P' located behind the mirror. According to the law of reflection, this image point is positioned at the same distance behind the mirror as the original object point is in front of it. As a result, an observer receiving these reflected rays, such as on their retina, perceives the point as if it were situated behind the mirror, even though no light actually travels behind the mirror surface.



(a)



(b)

Figure 6.1: Image formation on a plane mirror.

When multiple points of an object emit light towards the mirror, this principle applies to each point. As a result, the entire object appears as an image behind the mirror. Since each point of the image is equidistant from the mirror as its corresponding object point, the image has the same size as the object. This leads to the definition of magnification as:

$$M = \frac{h_{\text{image}}}{h_{\text{object}}}$$

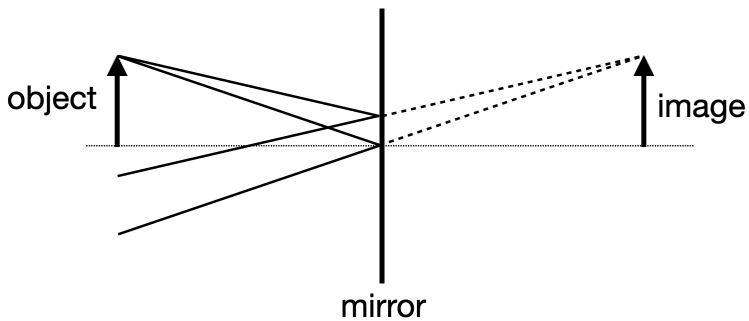


Figure 6.2: Image formation on a plane mirror.

i Virtual Images

A virtual image is an optical illusion where light rays appear to come from a point, but don't actually converge there. Unlike real images, virtual images can't be projected onto a screen. They're commonly seen in plane mirrors, convex mirrors, and when objects are closer to a lens than its focal point. **Remember:** for virtual images, light rays only seem to originate from the image when traced backwards.

i Real Images

A real image forms when light rays actually meet at a point after reflection or refraction. These images can be projected onto a screen because light physically passes through the image location. Real images are often inverted and occur with concave mirrors and lenses when objects are beyond the focal point. **Key point:** real images involve actual convergence of light rays.

6.1.2 Concave Mirrors

For a concave mirror (where the reflecting surface is on the inside of the spherical curve), applying the law of reflection yields interesting results. Light rays parallel to the optical axis, at a distance h from it, are reflected towards the axis and intersect it at a specific point F . Due to the mirror's symmetry, a parallel ray on the opposite side of the axis will also converge to this same point F .

We may calculate the position of the point F , e.g. the distance from the mirror surface point O , by applying the law of reflection. If the spherical mirror surface has a radius R , then the distance between the center of the sphere M and the point F is given by

$$FM = \frac{R}{2 \cos(\alpha)}$$

Therefore, we can also calculate the distance of the mirror surface from the point F , which results in

$$OF = R \left(1 - \frac{1}{2 \cos(\alpha)} \right) = f \quad (6.1)$$

This distance is the so-called focal length of the concave mirror f . For small angle α , the above equation yields the so called paraxial limit (all angles are small and the rays are close to the optical axis). In this limit we find $\cos(\alpha) \approx 1$ and the focal length becomes $f = R/2$. If we replace the cosine function by $\cos(\alpha) = \sqrt{1 - \sin^2(\alpha)}$ with $\sin(\alpha) = h/R$, we find

$$f = R \left[1 - \frac{R}{2\sqrt{R^2 - h^2}} \right] \quad (6.2)$$

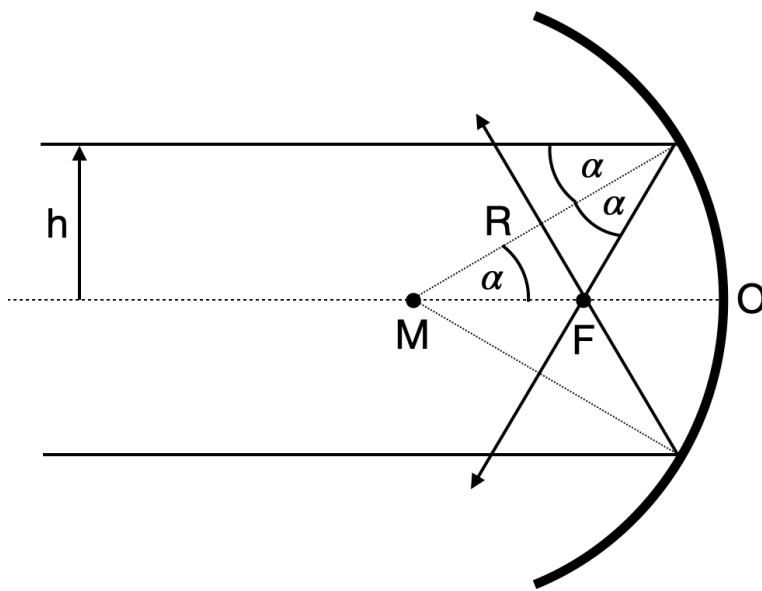


Figure 6.3: Reflection of a parallel ray incident at a height h from the optical axis on a concave mirror.

This equation is telling us, that the focal distance is not a single value for a concave mirror. The focal distance rather changes with the distance h from the optical axis. If h approaches R the focal length become shorter.

Focal Length of a Concave Spherical Mirror

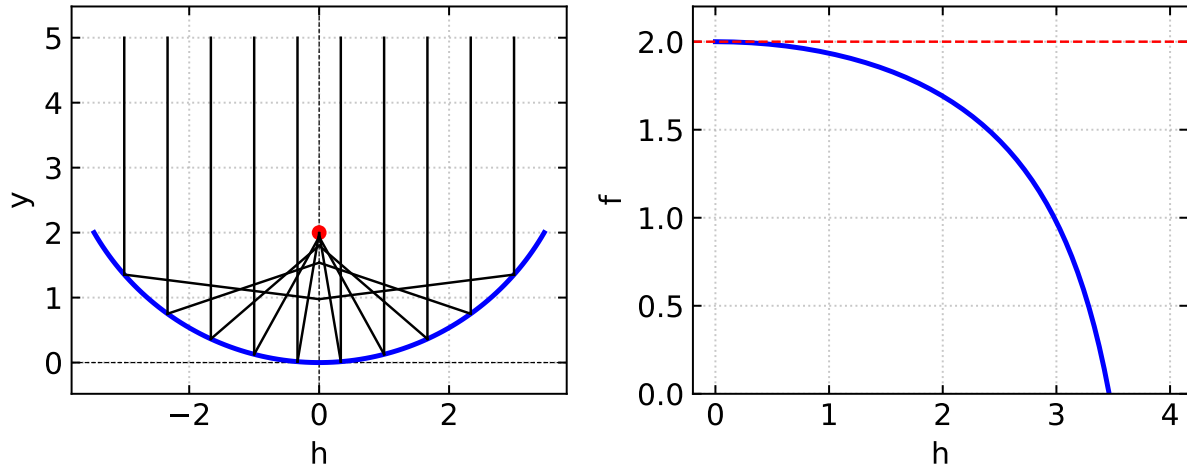


Figure 6.4: Spherical mirror of radius $R = 4$ reflecting parallel rays, showing spherical aberration and focal distance as a function of the distance from the optical axis h .

To obtain now an equation which predicts the point at which the reflected ray intersects the optical axis if it emerged at a point A , we just consider the following sketch.

For this situation, we can write down immediately the following relations

$$\delta = \alpha + \gamma$$

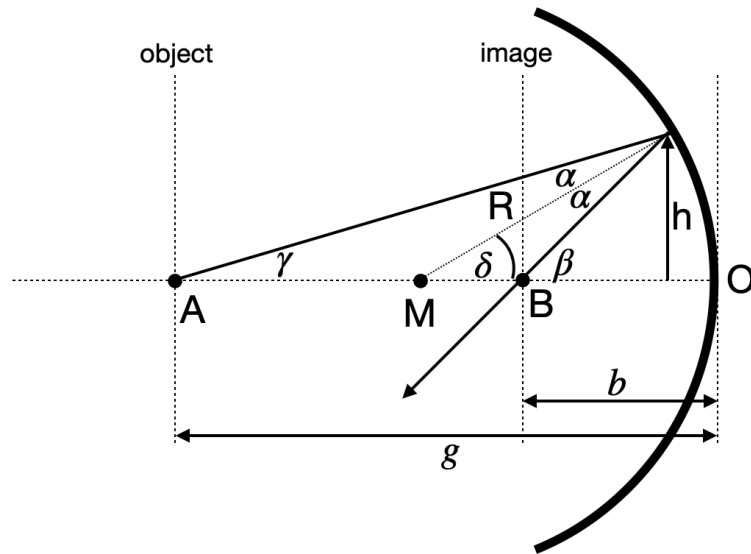


Figure 6.5: Image formation on a concave mirror.

$$\gamma + \beta = 2\delta$$

Further under the assumption of small angles (paraxial approximation) we can write down

$$\tan(\gamma) \approx \gamma = \frac{h}{g}$$

$$\tan(\beta) \approx \beta = \frac{h}{b}$$

$$\sin(\delta) \approx \delta = \frac{h}{R}$$

from which we obtain

$$\frac{h}{g} + \frac{h}{b} = 2\frac{h}{R}$$

and by dividing by h finally the imaging equation:

$$\frac{1}{g} + \frac{1}{b} = \frac{2}{R} = \frac{1}{f}$$

where we have used the focal length $f = R/2$. This equation has some surprising property. It is completely independent of h and γ . That means all points in a plane at a distance g are images into a plane at a distance b . Both planes are therefore called conjugated planes.

Imaging Equation Concave Mirror

The sum of the inverse object and image distances equals the inverse focal length of the concave mirror.

$$\frac{1}{g} + \frac{1}{b} \approx \frac{1}{f}$$

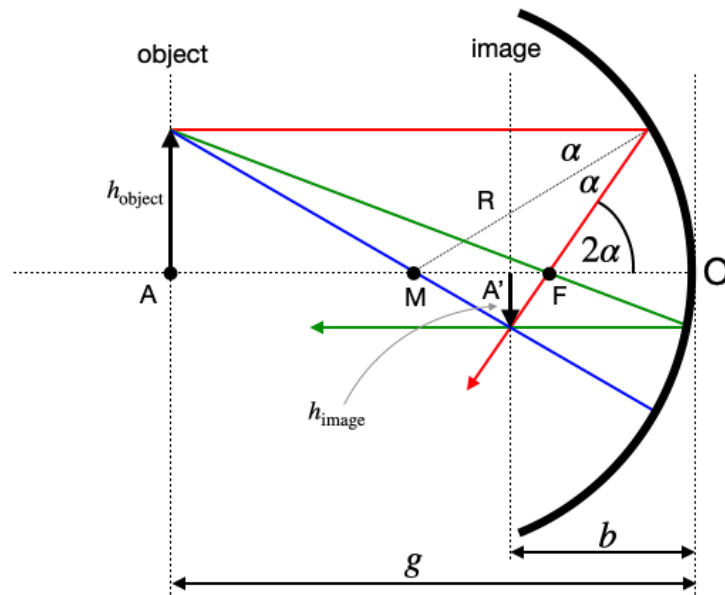


Figure 6.6: Image formation on a concave mirror.

This equation now helps to construct the image of an object in front of a concave mirror and we may define 3 different rays to identify the size of an image h_{image} from the size of an object h_{object} .

In the diagram above, three key rays are used to construct the image:

1. **Red ray:** Parallel to optical axis → reflects through focal point
2. **Green ray:** Through focal point → reflects parallel to optical axis
3. **Central ray:** Through center of curvature → reflects back along same path

The behavior of these reflected rays determines the nature of the image:

- If the rays intersect on the same side of the mirror as the object, a **real image** forms. This image is inverted, as shown in the sketch.
- If the rays diverge after reflection, they appear to intersect behind the mirror, creating a **virtual image**. This image is upright and located behind the mirror, though no actual ray intersection occurs.

The point where these rays meet (or appear to meet) determines the image size. By drawing a ray from the object's tip through the mirror's center (point O), we can easily determine the image height h_{image} . As an exercise, consider how this construction demonstrates that the magnification of a concave mirror is given by

$$\frac{h_{\text{image}}}{h_{\text{object}}} = -\frac{b}{g} = M$$

This ratio indeed represents the magnification M . The negative sign in the expression reflects an important optical property: for real images formed by concave mirrors, the image is inverted relative to the object. This inversion is mathematically represented by the negative magnification value. Conversely, a positive magnification would indicate an upright image, which occurs with virtual images.

With the help of the imaging equation and the magnification we may in general differentiate between the following general situations:

Object Distance	Image Characteristics	Image Position	Magnification
$g > 2f$	Real, inverted, smaller	Between f and 2f	$ m < 1$
$g = 2f$	Real, inverted, same size	At 2f	$ m = 1$

Object Distance	Image Characteristics	Image Position	Magnification
$f < g < 2f$	Real, inverted, larger	Beyond 2f	$ m > 1$
$g = f$	Image at infinity	At infinity	N/A
$g < f$	Virtual, upright, larger	Behind mirror	$ m > 1$

i Parabolic Mirrors Focus Parallel Rays

We would like to show in the following, that a parabolic mirror is a shape which reflects all light rays parallel to the principal axis to a single point, the focus. This is a fundamental property of parabolic mirrors and is used in many optical systems, such as telescopes, satellite dishes, and car headlights. For this purpose, we would like to use Fermat's principle. We examine a light ray originating from a point x, y_0 and travelling parallel to the principal axis. The light ray is reflected at a point (x, y) on the mirror and travels to the focus at $(0, p)$. The light path is therefore consisting out of two linear segments A and B for which we have to calculate the time of travel. The total duration of the light's journey is then:

$$t = t_A + t_B$$

where:

- t_A is the time taken to travel from x, y_0 to the mirror.
- t_B is the time taken to travel from (x, y) to $(0, p)$.

Time for Path A

The distance covered in path A is equal to $y_0 - y$, where y represents the y-coordinate of the point where the ray meets the mirror. Consequently, the time taken for the light to traverse path A can be expressed as:

$$t_A = \frac{y_0 - y}{c}$$

In this equation, c represents the speed of light in the medium.

Time for Path B

After reflection, the light ray travels from the point (x, y) on the mirror's surface to the focal point located at $(0, p)$. The length of this segment of the path can be calculated using the distance formula:

$$\sqrt{x^2 + (y - p)^2}$$

Consequently, the time required for the light to traverse path B is expressed as:

$$t_B = \frac{\sqrt{x^2 + (y - p)^2}}{c}$$

Total Time

The total time for the light ray's journey is the sum of times for paths A and B:

$$t = \frac{y_0 - y}{v} + \frac{\sqrt{x^2 + (y - p)^2}}{c}$$

According to Fermat's principle, all light rays should take the same time. We can express this by setting the total time equal to a constant t_c :

$$\frac{y_0 - y}{v} + \frac{\sqrt{x^2 + (y - p)^2}}{v} = t_c$$

For a ray traveling along the y-axis, reflecting at $(0, 0)$, the total distance is $y_0 + p$. The time for this ray is:

$$\frac{y_0 + p}{c}$$

This gives us $t_c = \frac{y_0 + p}{c}$. Substituting into our general equation:

$$\frac{y_0 - y}{v} + \frac{\sqrt{x^2 + (y - p)^2}}{c} = \frac{y_0 + p}{c}$$

Multiplying by c and rearranging:

$$y_0 - y + \sqrt{x^2 + (y - p)^2} = y_0 + p$$

$$\sqrt{x^2 + (y - p)^2} = y + p$$

Squaring both sides and simplifying:

$$x^2 + (y - p)^2 = (y + p)^2$$

$$x^2 + y^2 - 2py + p^2 = y^2 + 2py + p^2$$

$$x^2 = 4py$$

or

$$y = \frac{1}{4p}x^2$$

This final equation describes a parabola with its focus at $(0, p)$. The code below plots a parabolic mirror reflecting parallel rays to the focal point. Yet, I'm cheating a bit here. I'm not calculating the reflected rays, but just plotting them.

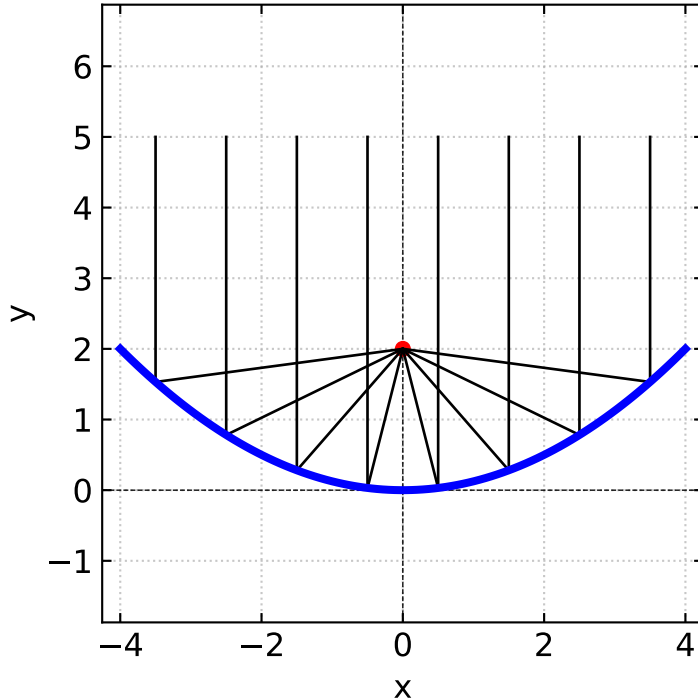


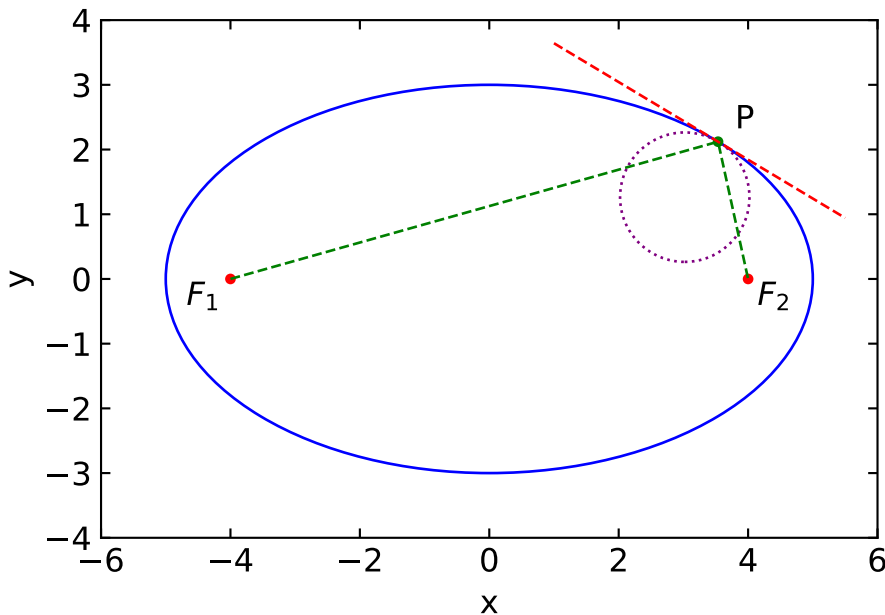
Figure 6.7: Parabolic mirror reflecting parallel rays to focal point

Elliptical Mirrors and Fermat's Principle

There is one interesting feature about elliptical mirrors: they can focus light from one focal point to the other. This is because the sum of the distances from any point on the ellipse to the two focal points is constant. This property is known as the **ellipse's geometric definition** and you can try that at home with a piece of string and two pins.

We can now apply Fermat's principle to proof that the light reflected from the ellipse travels a path length that is a saddle point. This means that the path length is stationary with respect to small perturbations in the path. Assuming for example that light travels from one focal point by a different path that is reflected from a line which is tangent to the ellipse at the point of reflection, the path length would be longer at any other point than the initial reflection point.

On the other side, if we reflect the ray on a surface that is a circle, which is intersecting the ellipse at the point of reflection, the path length would be shorter at any other point than the initial reflection point. This is a proof that the ellipse is a saddle point.



Mathematical Description

Ellipse Definition

Consider an ellipse with semi-major axis a and semi-minor axis b , defined by:

$$\frac{x^2}{a^2} + \frac{y^2}{b^2} = 1$$

Focal Points

The focal points are located at $F_1(-c, 0)$ and $F_2(c, 0)$, where:

$$c^2 = a^2 - b^2$$

Path Length

Let $P(x_0, y_0)$ be a point on the ellipse. The total path length L from F_1 to F_2 via P is:

$$L = |F_1P| + |PF_2| = \sqrt{(x_0 + c)^2 + y_0^2} + \sqrt{(x_0 - c)^2 + y_0^2}$$

Fermat's Principle

The path length L is stationary with respect to small perturbations in P :

$$\frac{\partial L}{\partial x_0} = 0 \quad \text{and} \quad \frac{\partial L}{\partial y_0} = 0 \quad \text{at the reflection point}$$

Tangent Line

The tangent line to the ellipse at $P(x_0, y_0)$ is given by:

$$\frac{x_0 x}{a^2} + \frac{y_0 y}{b^2} = 1$$

Let Q be any point on this tangent line different from P . The path $F_1 \rightarrow Q \rightarrow F_2$ is longer than $F_1 \rightarrow P \rightarrow F_2$:

$$|F_1 Q| + |Q F_2| > |F_1 P| + |P F_2|$$

Circle of Curvature

The radius of curvature R at P is:

$$R = \frac{(a^2 b^2)^{3/2}}{(b^2 x_0^2 + a^2 y_0^2)^{3/2}}$$

The center of curvature C is located at:

$$C = P + R \cdot \mathbf{n}$$

where \mathbf{n} is the unit normal vector at P .

Let Q be any point on this circle different from P . The path $F_1 \rightarrow Q \rightarrow F_2$ is shorter than $F_1 \rightarrow P \rightarrow F_2$:

$$|F_1 Q| + |Q F_2| < |F_1 P| + |P F_2|$$

As a consequence, the path length for the reflection on an ellipse between the two focal points must be a saddle point.

Chapter 7

Optical Elements Part II

7.1 Prism

Prisms are wedge-shaped optical elements made of a transparent material, such as glass. A special form of such a prism is an isosceles prism with two sides of equal length. The two equal sides enclose an angle γ , known as the apex angle of the prism. When light passes through this prism, it undergoes refraction twice.

First, the incident angle α_1 is changed into a refracted angle β_1 as the light enters the prism. This refracted ray then hits the second interface at an angle β_2 , leading to a second refraction as it exits the prism at an angle α_2 .

Of particular interest is the total deflection of the incident ray, which is measured by the angle δ . This deflection angle represents the difference between the final outgoing angle α_2 and the initial incident angle α_1 .

Understanding how this deflection angle changes based on the prism's properties and the incident angle is crucial in various optical applications. In the following sections, we will explore how to calculate this deflection angle and examine its dependence on different parameters.

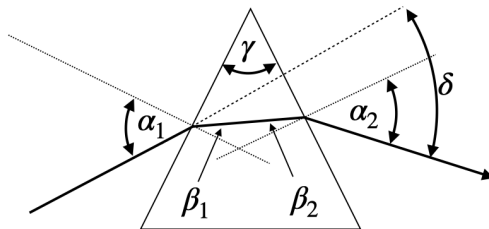


Figure 7.1: Refraction of rays on a prism.

7.1.1 Deflection angle

We can calculate the deflection angle δ from a number of considerations. First consider the following relations between the angles in the prism and Snell's law

$$\beta_1 = \sin^{-1} \left(\frac{n_0}{n_1} \sin(\alpha_1) \right)$$

$$\beta_2 = \gamma - \beta_1$$

$$\alpha_2 = \sin^{-1} \left(\frac{n_1}{n_0} \sin(\beta_2) \right)$$

$$\theta_2 = \alpha_2 - \gamma$$

where θ_2 is the angle between the incident surface normal and the outgoing ray. The total deflection angle δ is then

$$\delta = \alpha_1 - \beta_1 + \alpha_2 - \beta_2$$

or

$$\delta = \alpha_1 + \alpha_2 - \gamma$$

from which we obtain

$$\delta = \alpha_1 + \sin^{-1} \left(\frac{n_1}{n_0} \sin \left[\gamma - \sin^{-1} \left(\frac{n_0}{n_1} \sin(\alpha_1) \right) \right] \right) - \gamma$$

as the deflection angle.

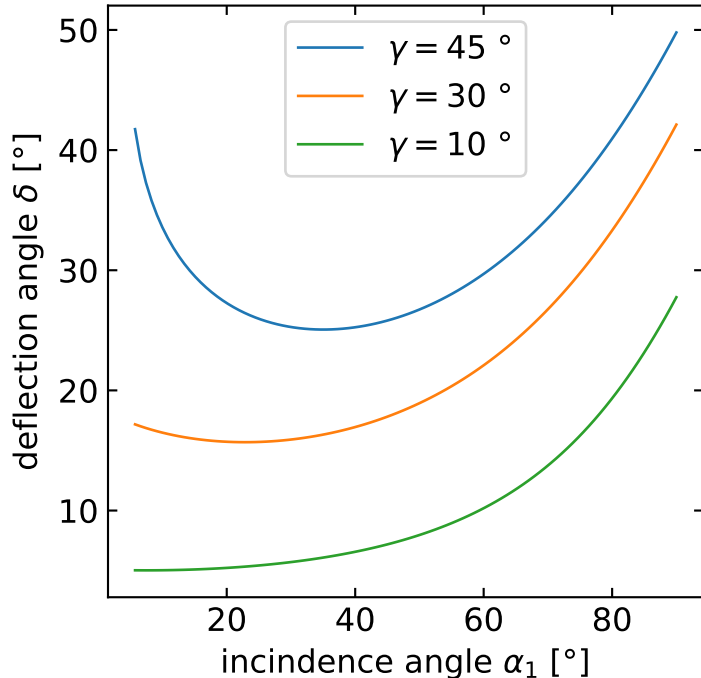


Figure 7.2: Deflection angle as a function of the incidence angle for different prism angles.

7.1.2 Minimum deflection angle

If we now would like to know how the deflection angle changes with the incident angle α_1 , we calculate the derivative of the deflection angle δ with respect to α_1 , i.e.,

$$\frac{d\delta}{d\alpha_1} = 1 + \frac{d\alpha_2}{d\alpha_1}.$$

We are here especially interested in the case, where this change in deflection is reaching a minimum, i.e., $d\delta/d\alpha_1 = 0$. This readily yields

$$d\alpha_2 = -d\alpha_1.$$

This means a change in the incidence angle $d\alpha_1$ yields an opposite change in the outgoing angle $-d\alpha_2$. We may later observe that in the experiment.

As both, the incident and the outgoing angle are related to each other by Snells's law, we may introduce the derivatives of Snell's law for both interfaces, e.g.,

- $\cos(\alpha_1)d\alpha_1 = n \cos(\beta_1)d\beta_1$
- $\cos(\alpha_2)d\alpha_2 = n \cos(\beta_2)d\beta_2$

where n is the refractive index of the prism material and the material outside is air ($n_{\text{air}} = 1$). Replacing $\cos(\alpha) = \sqrt{1 - \sin^2(\alpha)}$ and dividing the two previous equations by each other readily yields

$$\frac{1 - \sin^2(\alpha_1)}{1 - \sin^2(\alpha_2)} = \frac{n^2 - \sin^2(\alpha_1)}{n^2 - \sin^2(\alpha_2)}.$$

The latter equation is for $n \neq 1$ only satisfied if $\alpha_1 = \alpha_2 = \alpha$. In this case, the light path through the prism must be symmetric and we may write down the minimum deflection angle δ_{\min} :

Minimum prism deflection

The minimum deflection angle of an isosceles prism with a prism angle γ is given by

$$\delta_{\min} = 2\alpha - \gamma.$$

Given this minimum deflection angle δ_{\min} and the properties of the prism, we may also write down Snell's law using $\sin(\alpha) = n \sin(\beta)$, which results in

$$\sin\left(\frac{\delta_{\min} + \gamma}{2}\right) = n \sin\left(\frac{\gamma}{2}\right).$$

which indicates the dependence of the deflection in the refractive index n of the prism material.

7.1.3 Dispersion

Very important applications now arise from the fact, that the refractive index is a material property, which depends on the color (frequency or wavelength) of light. We do not yet understand the origin of this dependence. The plots below show the wavelength dependence of three different glasses. You may find much more data on the refractive index of different materials in an [online database](#).

The plots have a general feature, which is that the refractive index is largest at small wavelength (blue colors), while it drops continuously with increasing wavelength towards the red (800 nm). If you would characterize the dependence by the slope, i.e., $dn/d\lambda$ then all displayed curves show in the visible range

- $\frac{dn}{d\lambda} < 0$, is called normal dispersion

while

- $\frac{dn}{d\lambda} > 0$, is called anomalous dispersion

This wavelength dependence of the refractive index will yield a dependence of the deflection angle on the color of light as well. The change of the deflection angle with the refractive index can be calculated to be

$$\frac{d\delta}{dn} = \frac{2 \sin(\gamma/2)}{\sqrt{1 - n^2 \sin^2(\gamma/2)}}$$

together with the relation

$$\frac{d\delta}{d\lambda} = \frac{d\delta}{dn} \frac{dn}{d\lambda}$$

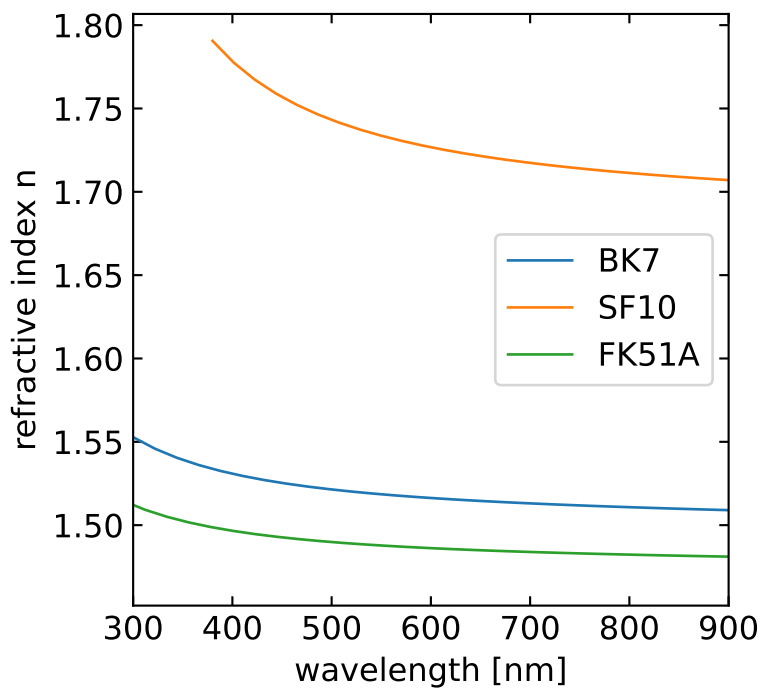


Figure 7.3: Refractive index of different glasses as a function of the wavelength.

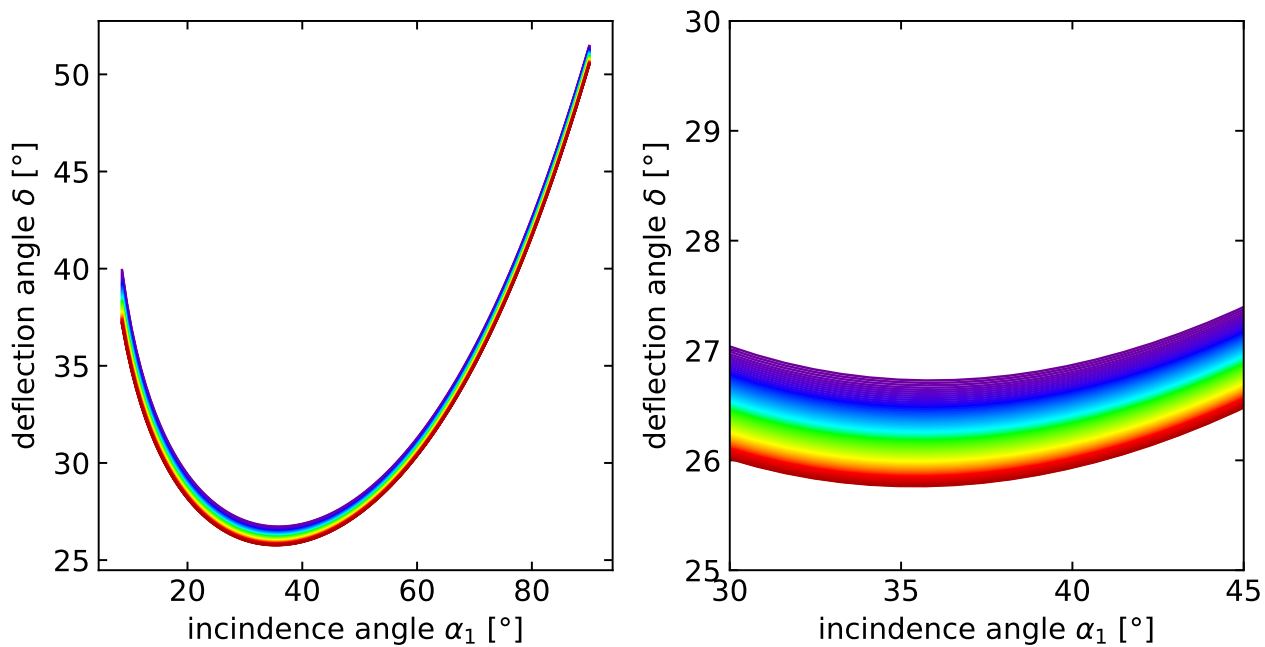


Figure 7.4: Deflection angle as a function of the incidence angle for different wavelengths.

we obtain

$$\frac{d\delta}{d\lambda} = \frac{2 \sin(\gamma/2)}{\sqrt{1 - n^2 \sin^2(\gamma/2)}} \frac{dn}{d\lambda}.$$

The refraction of white light through a prism splits the different colors composing white light spatially into a colored spectrum. In this process, light with the longest wavelength (red) is deflected the least, while light with the shortest wavelength (violet) is deflected the most. This occurs because the refractive index of the prism material varies with wavelength, a phenomenon known as dispersion.

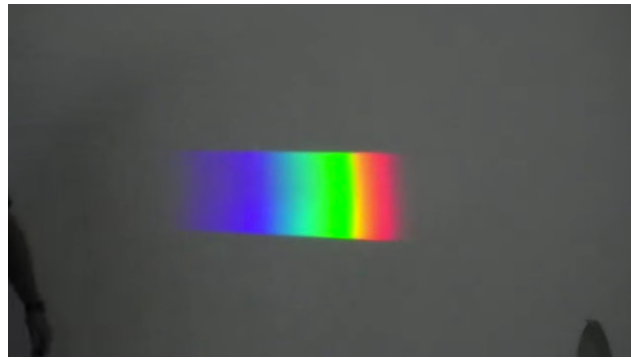
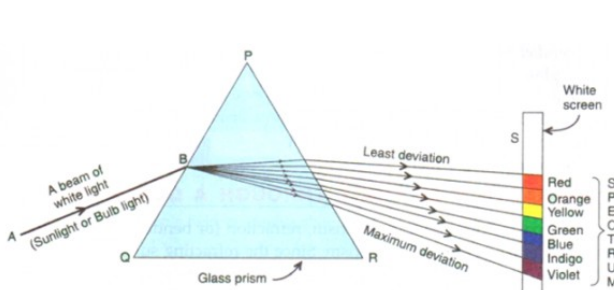


Figure 7.5: Spectrum as created by a prism in the lecture.



(a) Spectrum



(b) Prism

Figure 7.6: Deflection of different wavelengths of light in a prism with normal dispersion.

7.1.4 Prisms spectrograph

This wavelength-dependent refraction is crucial as it forms the basis for spectroscopy, a powerful analytical technique that measures and records the intensity of light as a function of wavelength. Spectroscopy allows scientists to analyze the composition and properties of matter by examining its interaction with light across different wavelengths.

DIY prism

If you don't have a prism at home (which most people don't), you can create a simple substitute using a mirror and a basin of water. Here's how:

1. Place a mirror in a basin of water, partially submerged.
2. Shine white light from a flashlight onto the mirror.
3. Observe the reflected and refracted light, paying special attention to the edges.

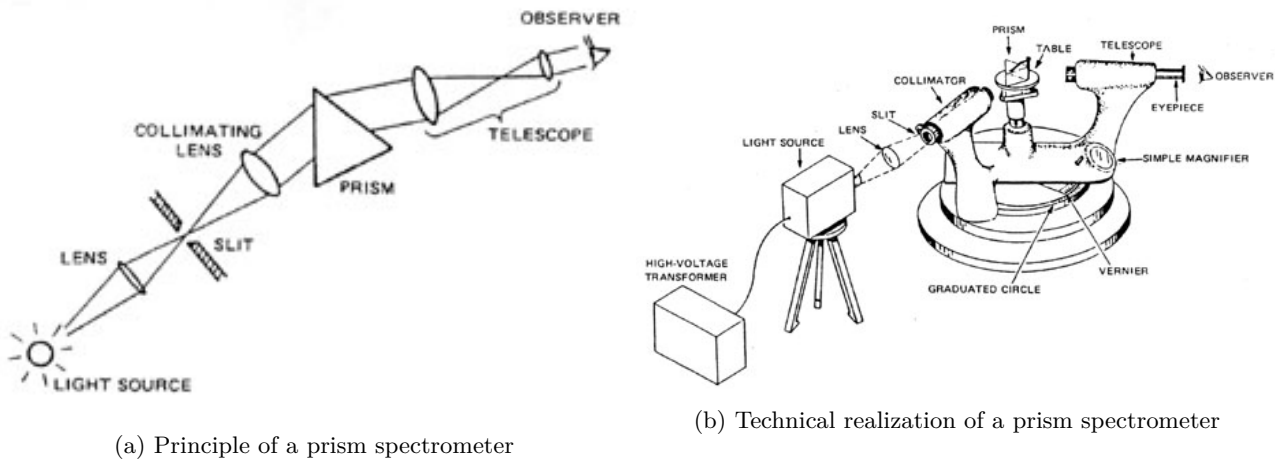


Figure 7.7: Principle and technical realization of a prism spectrometer.

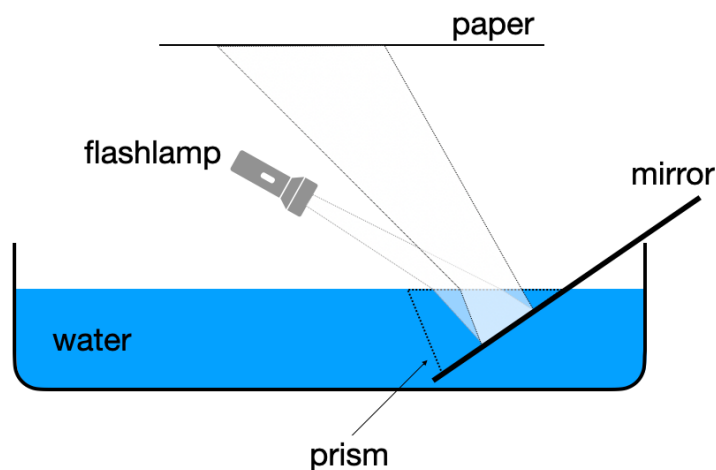


Figure 7.8: Home made water prism.

For better results, you can create a small aperture by making a tiny hole in a piece of black paper and placing it in front of the flashlight.

While the dependence of water's refractive index on wavelength is relatively weak, it's still sufficient to demonstrate the familiar colors of the rainbow. This phenomenon will be referenced later in our discussion.

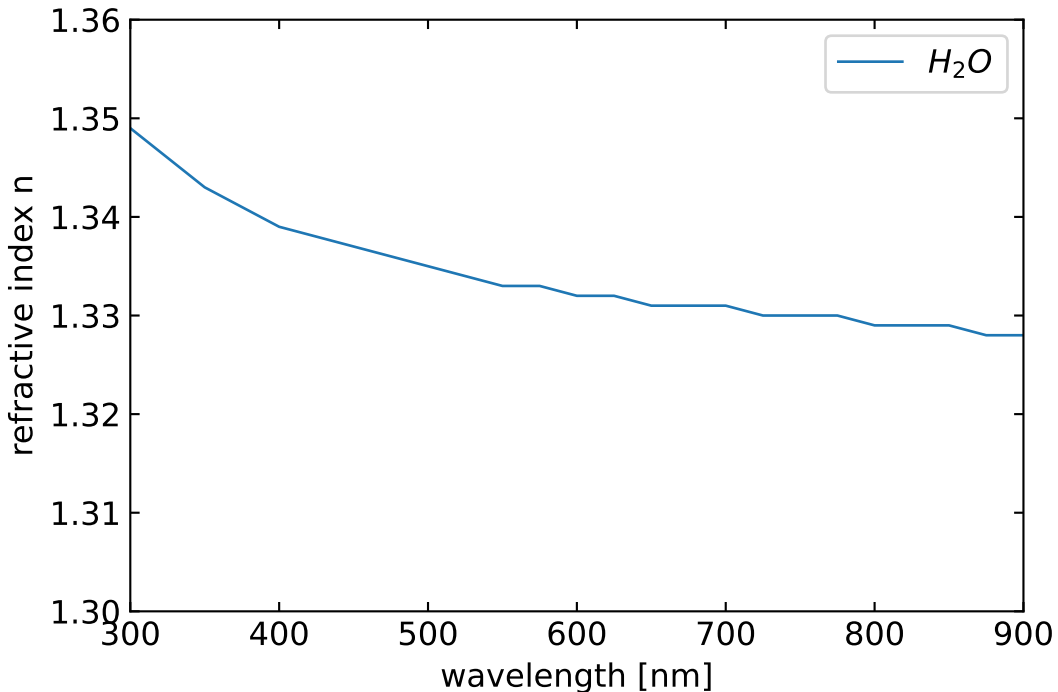


Figure 7.9: Refractive index of water as a function of the wavelength.

i Applications of prisms

Prisms are versatile optical components with a wide range of applications across various fields. Here are some common uses of prisms:

Binoculars and Telescopes:

Porro prisms in traditional binoculars and roof prisms in modern designs serve to correct image inversion and provide a compact form. These prisms enable a longer optical path within a shorter physical length, enhancing magnification while maintaining portability. This design is crucial for both binoculars and some telescopes, offering users powerful magnification in a handheld device.

Periscopes:

Right-angle prisms are the key component in periscopes, redirecting light at 90-degree angles. This simple yet effective design allows viewers to see over obstacles or around corners, making periscopes invaluable in submarines and various military applications where direct line of sight is obstructed.

Beam Splitting:

Cube beamsplitters play a vital role in dividing a single beam of light into two separate beams. This capability is essential in various scientific and medical applications, including interferometry, holography, and optical coherence tomography (OCT). The ability to split light beams precisely opens up numerous possibilities in research and diagnostics.

Beam Steering:

Risley prisms, consisting of a pair of rotating wedge prisms, offer precise control over laser beam direction. This technology finds applications in laser scanning, target tracking, and adaptive optics. The ability to steer beams accurately is crucial in fields ranging from military applications to advanced scientific research.

Digital Projectors:

Total Internal Reflection (TIR) prisms are a crucial component in Digital Light Processing (DLP) projectors. They direct light from the lamp to the Digital Micromirror Device (DMD) and then to the projection lens, enabling the high-quality image projection that DLP technology is known for.

Camera Systems:

In Single-Lens Reflex (SLR) cameras, pentaprism play a critical role in the viewfinder system. They flip the image from the lens to appear upright and correctly oriented in the viewfinder, allowing photographers to accurately compose their shots.

Laser Systems:

Brewster prisms find use in laser systems for polarization and wavelength separation. Additionally, dispersing prisms can be employed for wavelength tuning in certain laser setups, providing precise control over the laser's output characteristics.

Fiber Optic Communications:

In the realm of telecommunications, prisms are utilized in some fiber optic connectors and switches. They help redirect light between fibers, playing a crucial role in maintaining signal integrity and enabling complex network architectures.

Solar Energy:

Fresnel lenses, a specialized type of prism, are employed in concentrated solar power systems. These lenses focus sunlight efficiently, contributing to the development of more effective solar energy collection technologies.

Head-Up Displays (HUDs):

Prisms are an integral part of HUD systems in both automotive and aviation contexts. They project crucial information onto the windshield or a combiner glass, allowing drivers or pilots to access important data without taking their eyes off their primary viewpoint.

Microscopy:

Nomarski prisms enhance the capabilities of differential interference contrast microscopy. They increase contrast in transparent specimens, enabling scientists to observe details that would be difficult or impossible to see with conventional microscopy techniques.

Optical Coherence Tomography (OCT):

In some OCT systems, prisms are employed for sample arm scanning and reference arm delay. This application of prisms contributes to the high-resolution imaging capabilities of OCT, which is particularly valuable in medical diagnostics, especially in ophthalmology.

Chapter 8

Optical Elements Part III

8.0.1 Lenses

The most important optical elements are lenses, which come in many different flavors. They consist of curved surfaces, which most commonly have the shape of a part of a spherical cap. It is, therefore, useful to have a look at the refraction at spherical surfaces.

Refraction at spherical surfaces

For our calculations of the refraction at spherical surfaces, we consider the sketch below.

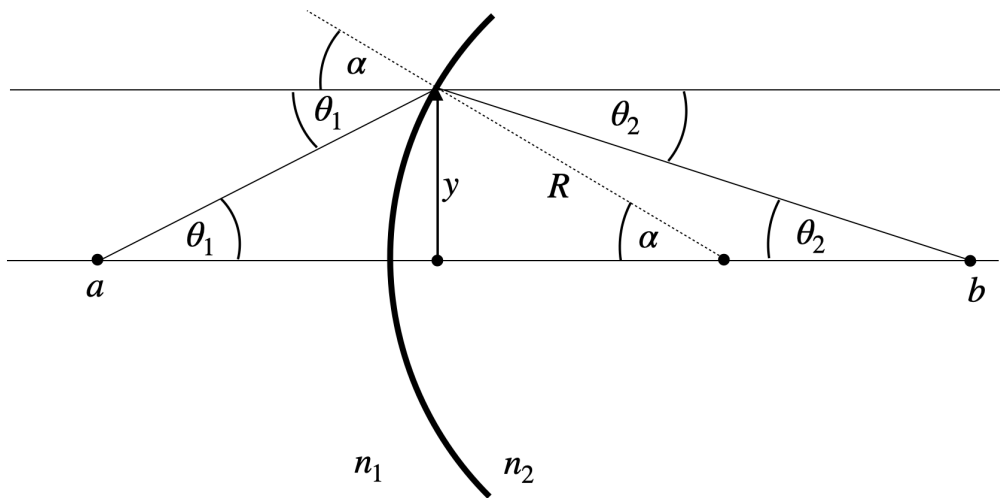


Figure 8.1: Refraction at a curved surface.

To derive an imaging equation for a lens, we aim to calculate the distance b and angle θ_2 at which a ray crosses the optical axis, given its origin at distance a and angle θ_1 . We begin with Snell's law for the geometry:

$$n_1 \sin(\alpha + \theta_1) = n_2 \sin(\alpha - \theta_2)$$

We define key relationships:

$$\sin(\alpha) = \frac{y}{R}, \quad \tan(\theta_1) = \frac{y}{a}, \quad \tan(\theta_2) = \frac{y}{b}$$

To simplify this, we employ the **paraxial approximation**, which assumes all angles are small. This allows us to use first-order approximations of trigonometric functions, effectively linearizing them:

$$\sin(\theta) \approx \theta + O(\theta^3), \quad \tan(\theta) \approx \theta + O(\theta^3), \quad \cos(\theta) \approx 1 + O(\theta^2)$$

This approach, common in optics, significantly simplifies our calculations while maintaining accuracy for most practical scenarios involving lenses.

With the help of these approximations we can write Snell's law for the curved surface as

$$n_1(\alpha + \theta_1) = n_2(\alpha - \theta_2).$$

With some slight transformation which you will find in the video of the online lecture we obtain, therefore,

$$\theta_2 = \frac{n_2 - n_1}{n_2 R} y - \frac{n_1}{n_2} \theta_1,$$

which is a purely linear equation in y and θ_1 .

Paraxial Approximation

The paraxial approximation is a fundamental simplification in optics that assumes all angles are small. This allows us to use linear approximations for trigonometric functions, significantly simplifying calculations while maintaining accuracy for most practical scenarios involving lenses.

To visualize the validity of this approximation, let's examine two plots:

1. The first plot compares $\sin(\theta)$ (blue line) with its linear approximation (red dashed line) for angles ranging from 0 to $\pi/2$ radians.
2. The second plot shows the absolute error between $\sin(\theta)$ and the linear approximation.

These plots demonstrate that:

1. For small angles (roughly up to 0.5 radians or about 30 degrees), the approximation is very close to the actual sine function.
 2. The error increases rapidly for larger angles, indicating the limitations of the paraxial approximation.
- In most optical systems, especially those involving lenses, the angles of incident and refracted rays are typically small enough for this approximation to be valid. However, it's important to be aware of its limitations when dealing with wide-angle optical systems or scenarios where precision is critical.

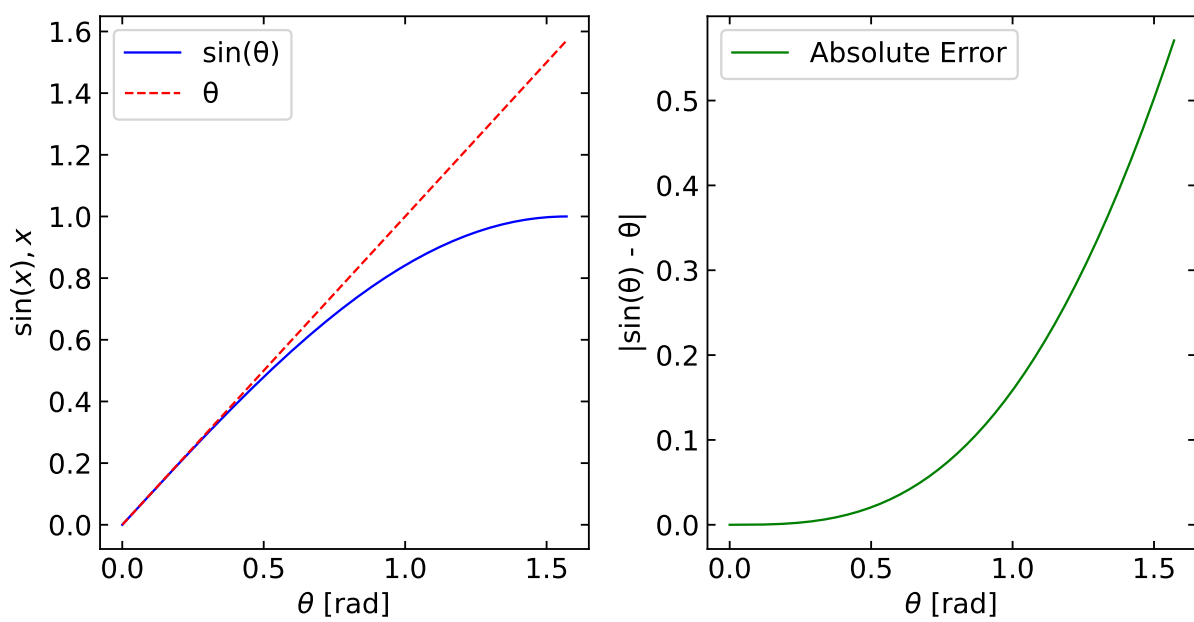


Figure 8.2: Visualization of the paraxial approximation plotting the $\sin(\theta)$ and the linear approximation θ (dashed line) for angles ranging from 0 to $\pi/2$ radians.

Consider light originating from a point at distance y from the optical axis. We'll analyze two rays: one traveling parallel to the optical axis and hitting the spherical surface at height y , and another incident at $y = 0$.

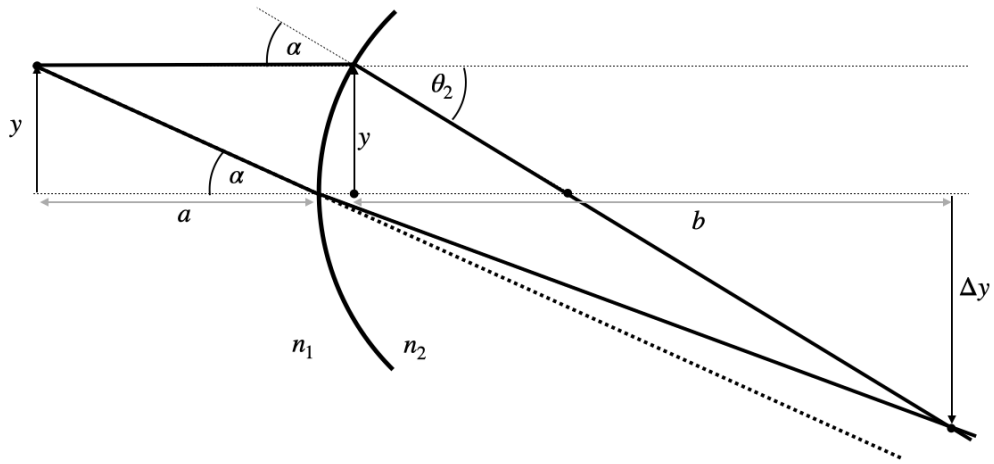


Figure 8.3: Image formation at a curved surface.

Applying our derived formula to these two cases:

For the parallel ray ($\theta_1 = 0$):

$$\theta_2 = \frac{n_2 - n_1}{n_2} \frac{y}{R}$$

$$\theta_2 = \frac{y + \Delta y}{b}$$

Equating these expressions:

$$\frac{y + \Delta y}{b} = \frac{n_2 - n_1}{n_2} \frac{y}{R}$$

For the ray through the center ($y = 0$):

$$n_2 \frac{\Delta y}{b} = n_1 \frac{y}{a}$$

Combining these equations yields the imaging equation for a curved surface:

$$\frac{n_1}{a} + \frac{n_2}{b} = \frac{n_2 - n_1}{R}$$

We can define a new quantity, the **focal length**, which depends only on the properties of the curved surface:

$$f = \frac{n_2}{n_2 - n_1} R$$

Imaging Equation for Spherical Refracting Surface

The sum of the inverse object and image distances equals the inverse focal length of the spherical refracting surface:

$$\frac{n_1}{a} + \frac{n_2}{b} \approx \frac{n_2}{f}$$

where the focal length of the refracting surface is given by:

$$f = \frac{n_2}{n_2 - n_1} R$$

in the paraxial approximation.

8.0.2 Thin lens

In our previous calculation we have found a linear relation between the incident angle θ_1 with the optical axis, the incident height of the ray y and the outgoing angle θ_2 :

Analyzing refraction in a lens involves two spherical surfaces. Light initially travels from a medium with refractive index n_1 into the lens material with index n_2 . The first surface's radius, R_1 , is typically positive for a convex surface facing the incident light.

At the second surface, the outgoing angle from the first refraction becomes the incident angle for the second refraction. Here, light travels from n_2 back into n_1 . The radius R_2 of this surface often has a negative value in a converging lens due to its opposite curvature relative to the optical axis.

For thin lenses, where the thickness d is much smaller than R_1 and R_2 ($d \ll R_1, R_2$), we can simplify our analysis. We assume that the height of the ray at both surfaces is approximately equal ($y \approx y'$), neglecting the displacement inside the lens.

This simplification allows us to treat all refraction as occurring on a single plane at the lens center, known as the **principal plane**. This concept, illustrated by the dashed line in the figure, greatly simplifies optical calculations and ray tracing for thin lenses.

The radii's sign convention (positive for convex surfaces facing incident light, negative for concave) and this two-surface analysis form the basis for the thin lens formula. This formula relates object distance, image distance, and focal length, encapsulating the lens's imaging properties.

The result of the above calculation is leading to the imaging equation for the thin lens.

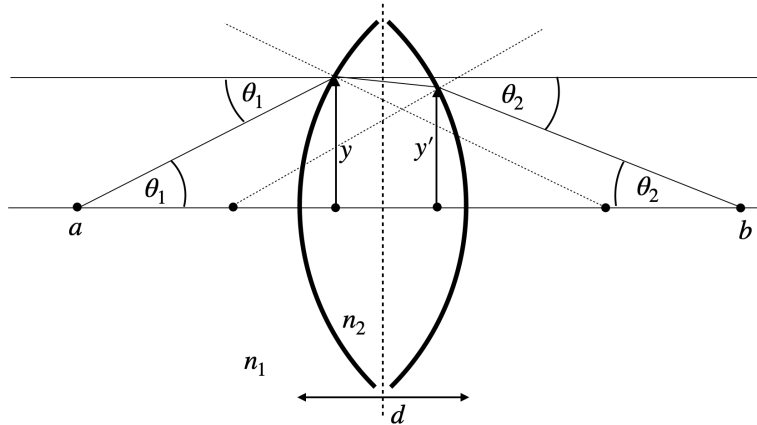


Figure 8.4: Refraction on two spherical surfaces.

i Imaging Equation for Thin Lens

The sum of the inverse object and image distances equals the inverse focal length of the thin lens:

$$\frac{1}{a} + \frac{1}{b} \approx \frac{n_2 - n_1}{n_1} \left(\frac{1}{R_1} - \frac{1}{R_2} \right) = \frac{1}{f}$$

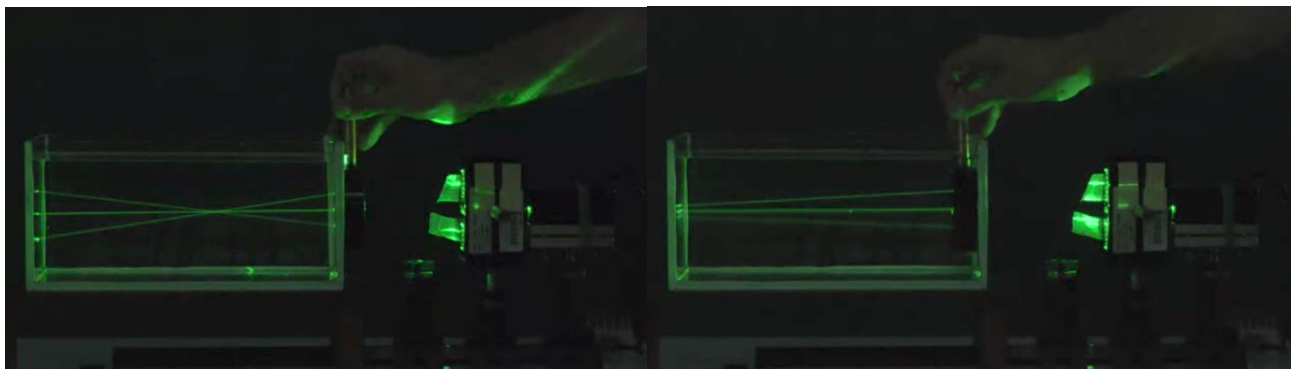
i Lensmaker equation

The focal length of a thin lens is calculated by the **lensmaker equation**:

$$f = \frac{n_1}{n_2 - n_1} \left(\frac{R_1 R_2}{R_2 - R_1} \right)$$

in the paraxial approximation.

The equation for the focal length has some important consequence. It says that if the difference of the refractive indices inside (n_2) and outside n_1 get smaller, the focal length becomes larger and finally infinity. This can be nicely observed by placing a lens outside and inside a water filled basin as shown below.



(a) Lens in air

(b) Lens in water

Figure 8.5: Focusing of parallel rays by a lens in air ($n_1 = 1$, left) and in water ($n_1 = 1.33$, right). The images clearly show the change in focal length between the two situations.

Bessel's method to measure the focal length of a lens

The is an interesting way to measure the focal length of a lens. Fix a distance D between object and screen. Then place a converging lens between them. Due to the reversibility of the light path, the lens will create a sharp image on the screen at two positions, which are separated by a distance d .

The equation for the focal distance can then be obtained from the

- Lens equation: $\frac{1}{f} = \frac{1}{a} + \frac{1}{b}$
- Total distance: $D = a + b$

Where f is focal length, a is object distance, and b is image distance. To obtain the focal distance according to this method, which is called the **Bessel method**, the following steps are taken:

For the first lens position:

$$D = a_1 + b_1$$

For the second lens position:

$$D = a_2 + b_2$$

We can further calculate the distance between the two lens positions:

$$d = a_1 - a_2 = b_2 - b_1$$

and use the imaging equation to find the focal length:

$$\frac{1}{f} = \frac{1}{a_1} + \frac{1}{b_1} = \frac{1}{a_2} + \frac{1}{b_2}$$

Substituting $b_1 = D - a_1$ and $b_2 = D - a_2$ we get further

$$\frac{1}{f} = \frac{1}{a_1} + \frac{1}{D - a_1} = \frac{1}{a_2} + \frac{1}{D - a_2}$$

Both euqations can be solved by

$$a_1 = \frac{D + d}{2} \quad \text{and} \quad a_2 = \frac{D - d}{2}$$

If we substitute that back into the imaging equation we obtain

$$\frac{1}{f} = \frac{2}{D} + \frac{2}{d}$$

which can be rearranged to get Bessel's formula:

$$f = \frac{D^2 - d^2}{4D}$$

This method only requires measuring D (fixed distance) and d (distance between lens positions). It eliminates the need to know exact object or image distances from the lens, making it more accurate than methods requiring precise distance measurements from the lens.

Image Construction

Images of objects can be now constructed if we refer to rays which do not emerge from a position on the optical axis only. In this case, we consider three different rays (two are actually enough). If we use as in the case of a concave mirror a central and a parallel ray, we will find a position where all rays cross on the other side. The conversion of the rays is exactly the same as in the case of a spherical mirror. The relation between the position of the object and the image along the optical axis is described by the imaging equation.

Similar to the concave mirror, we may now also find out the image size or the magnification of the lens.

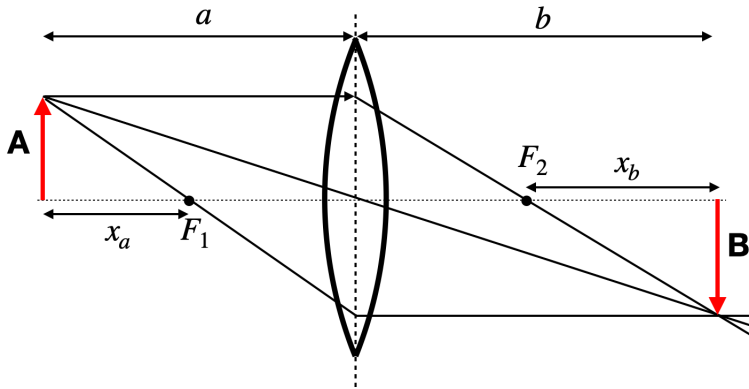


Figure 8.6: Image construction on a thin lens.

i Magnification of a Lens

The magnification is given by:

$$M = \frac{h_{\text{image}}}{h_{\text{object}}} = -\frac{b}{a} = \frac{f}{f-a}$$

where the negative sign is the result of the reverse orientation of the real images created by a lens.

According to our previous consideration $M < 0$ corresponds to a reversed image, while it is upright as the object for $M > 0$. We, therefore, easily see the following:

Object Position	Image Characteristics	Magnification (M)	Image Type
$a < f$	Upright and magnified	$M > 0$	Virtual
$f < a < 2f$	Reversed and magnified	$M < -1$	Real
$a = 2f$	Reversed, same size	$M = -1$	Real
$a > 2f$	Reversed and shrunk	$-1 < M < 0$	Real
$a = f$	Appears at infinity	$M = \infty$	-

The image below illustrates the construction of images in 4 of the above cases for a bi-convex lens with a parallel and a central ray for different object distances.

Fig.: Image construction on a biconvex lens with a parallel and a central ray for different object distances.

8.0.3 Thick lens

For a thin lens, the displacement of the beam in height (y, y') due to the thickness has been neglected. That means that we can reduce all refracting action of the lens to a single plane, which we call a principle plane. This approximation is (independent of the paraxial approximation) not anymore true for lenses if the displacement Δ of the ray as in the image below cannot be neglected. Such lenses are called **thick lenses** and they do not have a single principle plane anymore. In fact, the principle plane splits up into two principle planes at a distance h .

As indicated in the sketch above, an incident ray which is not deflected can be extended to its intersection with the optical axis at a point, which is a distance h_1 behind the lens surface. This is the location for the first principle plane. The position of the second principle plane at a distance h_2 before the back surface is found for by reversing the ray path. According to that, both principle planes have a distance $h = d - h_1 + h_2$ (mind the sign of the h). Using some mathematical effort, one can show that the same imaging equation as for a thins lens can be used with a new definition of the focal length and taking into account that object and image distances refer to their principle planes.

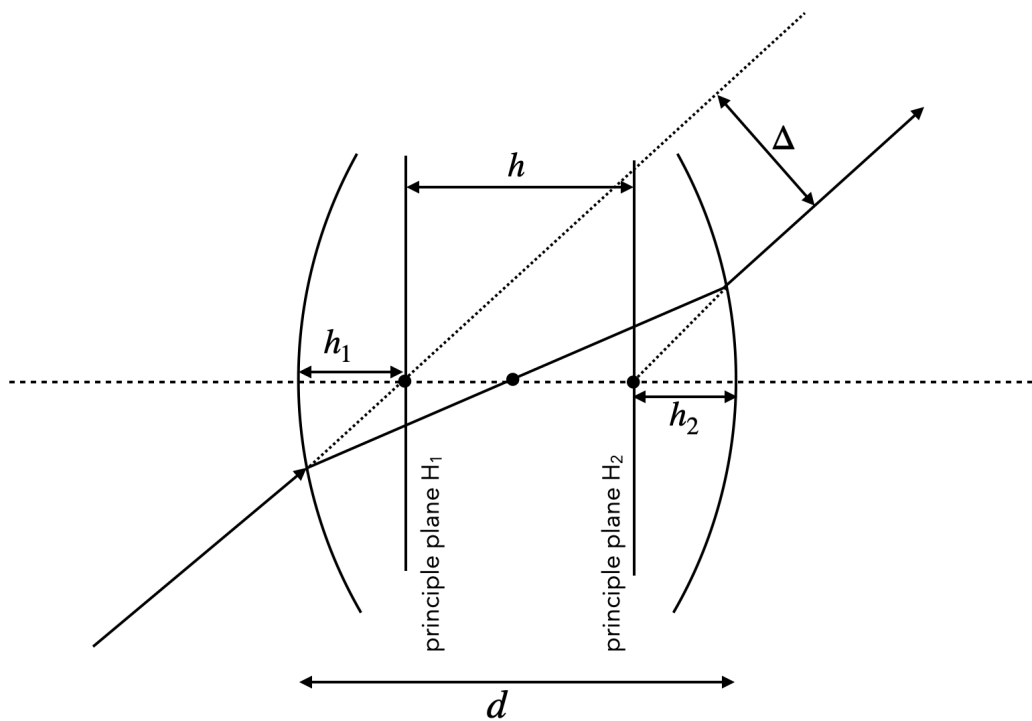


Figure 8.7: Thick lens principal planes.

Matrix Optics

The above derived equations for a single spherical surface yield a linear relation between the input variables y_1 and θ_1 and the output variables y_2 and θ_2 . The linear relation yields a great opportunity to express optical elements in terms of linear transformations (matrices). This is the basis of **matrix optics**. The matrix representation of a lens is given by

$$\begin{pmatrix} y_2 \\ \theta_2 \end{pmatrix} = \begin{pmatrix} 1 & 0 \\ -\frac{1}{f} & 1 \end{pmatrix} \begin{pmatrix} y_1 \\ \theta_1 \end{pmatrix}$$

where the matrix is called the **ABCD matrix** of the lens. Due to the linearization of Snells law we can write down more generally

$$\begin{pmatrix} y_2 \\ \theta_2 \end{pmatrix} = \begin{pmatrix} A & B \\ C & D \end{pmatrix} \begin{pmatrix} y_1 \\ \theta_1 \end{pmatrix}$$

and one can obtain a Matrix for all types of optical elements such as free space of distance d .

$$\begin{bmatrix} A & B \\ C & D \end{bmatrix} = \begin{bmatrix} 1 & d \\ 0 & 1 \end{bmatrix}$$

Here are some useful matrices for optical elements:

$$\mathbf{M} = \begin{bmatrix} 1 & d \\ 0 & 1 \end{bmatrix} \quad (\text{Free space})$$

$$\mathbf{M} = \begin{bmatrix} 1 & 0 \\ 0 & \frac{n_1}{n_2} \end{bmatrix} \quad (\text{Planar interface})$$

$$\mathbf{M} = \begin{bmatrix} 1 & 0 \\ -\frac{(n_2-n_1)}{n_2 R} & \frac{n_1}{n_2} \end{bmatrix} \quad (\text{Spherical Boundary})$$

$$\mathbf{M} = \begin{bmatrix} 1 & 0 \\ -\frac{1}{f} & 1 \end{bmatrix} \quad (\text{Tin Lens})$$

If we have now a system of optical elements, we can multiply the matrices of the individual elements to obtain the matrix of the whole system.

$$\rightarrow \mathbf{M}_1 \rightarrow \mathbf{M}_2 \rightarrow \mathbf{M}_N \rightarrow \mathbf{M} = \mathbf{M}_N \dots \mathbf{M}_2 \mathbf{M}_1.$$

This is a very powerful tool to analyze optical systems.

i Thick Lens Focal Length

We would like to model the imaging properties of a thick lens using the matrix method. The lens is divided into three components:

1. A thin lens at the front surface
2. A region of free space propagation through the lens material of thickness d
3. Another thin lens at the back surface

The matrices for these components are:

$$\mathbf{M}_1 = \begin{bmatrix} 1 & 0 \\ -1/f_1 & 1 \end{bmatrix}, \quad \mathbf{M}_2 = \begin{bmatrix} 1 & d \\ 0 & 1 \end{bmatrix}, \quad \mathbf{M}_3 = \begin{bmatrix} 1 & 0 \\ -1/f_2 & 1 \end{bmatrix}$$

Where - f_1 and f_2 are the focal lengths of the front and back surfaces, which are determined by the radii of curvature R_1 and R_2 of the surfaces - d is the thickness of the lens, measured along the optical axis

8.1 Derivation

For a lens with refractive index n in air, the focal lengths of the surfaces are:

$$\frac{1}{f_1} = \frac{n-1}{R_1}, \quad \frac{1}{f_2} = \frac{1-n}{R_2}$$

Where R_1 and R_2 are the radii of curvature of the front and back surfaces.

The total system matrix is then

$$\mathbf{M}_{total} = \mathbf{M}_3 \cdot \mathbf{M}_2 \cdot \mathbf{M}_1$$

After multiplication, the element in the lower left corner of the resulting matrix represents $-1/f$ for the entire lens system:

$$-\frac{1}{f} = -\frac{1}{f_2} - \frac{1}{f_1} + \frac{d}{f_1 f_2}$$

Substituting the expressions for $1/f_1$ and $1/f_2$:

$$\frac{1}{f} = \frac{n-1}{R_1} + \frac{n-1}{R_2} - \frac{d(n-1)^2}{nR_1 R_2}$$

Factoring out $(n-1)$:

$$\frac{1}{f} = (n-1) \left[\frac{1}{R_1} + \frac{1}{R_2} - \frac{(n-1)d}{nR_1 R_2} \right]$$

Rearranging slightly:

$$\frac{1}{f} = (n-1) \left[\frac{1}{R_1} - \frac{1}{R_2} + \frac{(n-1)d}{nR_1 R_2} \right]$$

This is the Lensmaker's equation for a thick lens.

The construction of ray diagrams for thick lenses is similar to that for thin lenses, but the object and image distances are measured from the principal planes. The magnification is also calculated using the distances from the principal planes. **Principal planes are where a thick lens can be treated as an equivalent thin lens. At these planes, the magnification is unity.**

The derivation of the location of the principle planes will be part of the seminar.

i Imaging Equation for Thick Lens

The sum of the inverse object and image distances to the principal planes (H_1, H_2) equals the inverse focal length of the thick lens:

$$\frac{1}{a} + \frac{1}{b} \approx \frac{1}{f}, \quad \text{where} \quad \frac{1}{f} = n - 1 \left(\frac{1}{R_1} - \frac{1}{R_2} + \frac{(n-1)d}{nR_1 R_2} \right)$$

in the paraxial approximation. The construction of the image on a thick lens is done with the help of two principle planes. The object distance a and the image distance b are measured from these principle planes. The location of the two principle planes are found to be

$$h_1 = -\frac{(n-1)fd}{nR_2}$$

$$h_2 = -\frac{(n-1)fd}{nR_1}$$

As compared to the construction of an image on a thin lens, we now have to consider some peculiarities for the thick lens. An incident parallel ray, which turns into a focal ray is now refracted at the second principle plane. The reverse must, therefore, be true for an incident focal ray. This ray is refracted on the first principle plane. The central ray is deflected on both principle planes. It is incident under a certain angle at the first principle plane and outgoing with the same principle angle to the second principle plane. The sketch below summarizes these issues for a thick lens.

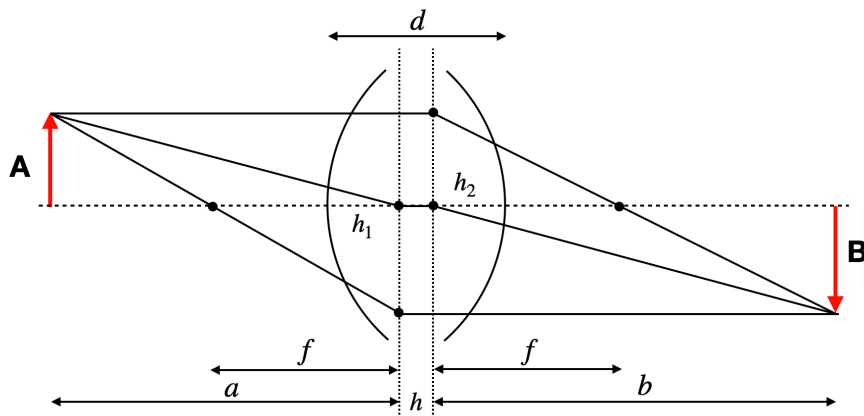


Figure 8.8: Thick lens image construction.

8.1.1 Lens types

Depending on the radii of curvature and their sign, one can construct different types of lenses that are used in many applications. Modern microscopy lenses, for example, can contain up to 20 different lenses, each with carefully designed curvatures and materials to correct for various optical aberrations and achieve high-quality imaging.

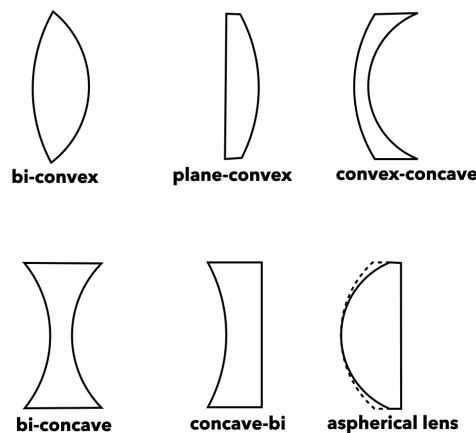


Figure 8.9: Different lens types.

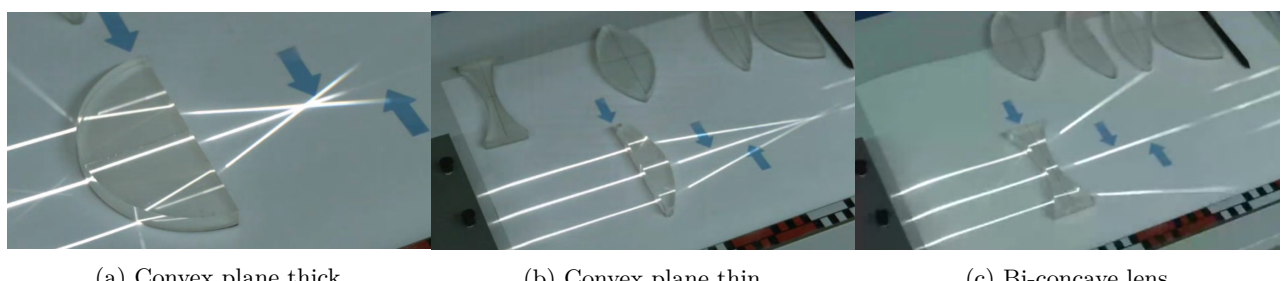


Figure 8.10: Focusing behavior of a few different lens types.

Chapter 9

Optical Instruments

9.1 The Human Eye

The human eye stands is one of the most remarkable sensory systems. This sophisticated organ combines an array of precisely crafted components—including an adjustable aperture, an adaptive lens, and a highly sensitive photodetector—all interconnected with a neural network capable of rapid and accurate pattern recognition. What's truly astounding is that this entire system operates on mere watts of power.

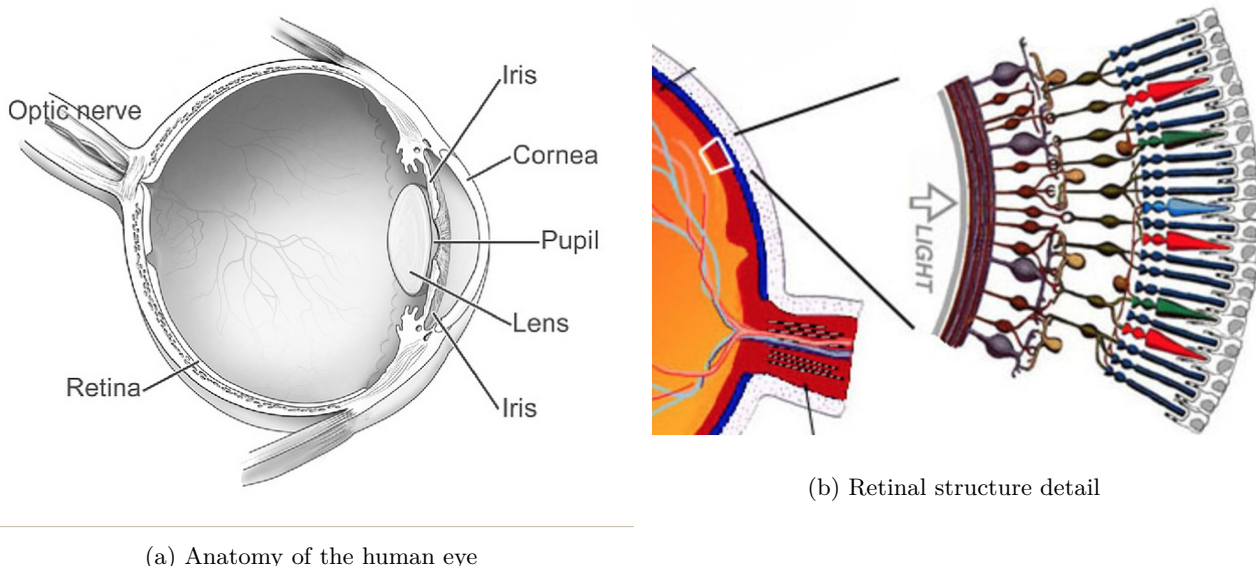


Figure 9.1: Left: Key components of the human eye, including the lens, vitreous body, and retina with its light-sensitive cells. Right: Detailed view of the retina, showing the arrangement and neural connections of rods and cones.

9.1.1 Key Components and Their Functions

1. **Pupil and Iris:** The pupil, surrounded by the iris, acts as an adjustable aperture. It regulates the amount of light entering the eye and influences the depth of field. In bright conditions, a constricted pupil increases the depth of field, allowing a wider range of distances to be in focus simultaneously.
2. **Lens:** Connected to the ciliary muscles, the lens can change its curvature to adjust focal length, a process known as accommodation. This allows the eye to focus on objects at varying distances.

3. **Vitreous Humor:** This gel-like substance fills the eye cavity, maintaining its shape and contributing to the eye's optical properties.
4. **Retina:** The light-sensitive layer at the back of the eye, containing photoreceptor cells (rods and cones) that convert light into neural signals.

9.1.2 Optical Properties of the Eye

The eye's optical system is asymmetrical due to the different media it interfaces with (air on one side, vitreous humor on the other). This results in different focal lengths:

- Front focal length: $f_1 = 17 \text{ mm}$
- Back focal length: $f_2 = 22 \text{ mm}$

These values can change during accommodation for near vision:

- Close object front focal length: $f_1 = 14 \text{ mm}$
- Close object back focal length: $f_2 = 19 \text{ mm}$

The eye's refractive power, measured in diopters (D), is the reciprocal of the focal length in meters. For a relaxed eye:

$$P = \frac{1}{f} = \frac{1}{0.022 \text{ m}} \approx 45.45 \text{ D}$$

During accommodation, this can increase to about 52 D.

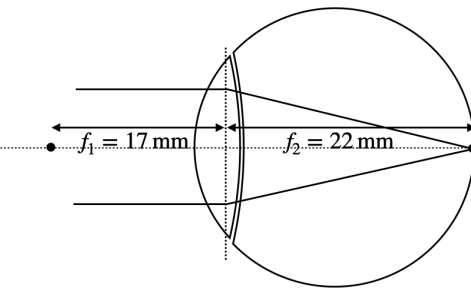


Figure 9.2: Illustration of the eye's focal distances.

9.1.3 Photoreceptors: Cones and Rods

The retina contains two types of photoreceptor cells:

1. **Cones:** Responsible for color vision and high acuity in bright light. They are concentrated around the fovea, the area of highest visual acuity.
2. **Rods:** More sensitive to light but do not distinguish colors, providing vision in low light conditions.

Cones contain light-sensitive pigments based on retinal molecules, which undergo conformational changes when excited by light, triggering a cascade of chemical processes. There are three types of cones, each sensitive to different wavelengths of light, enabling color vision.

9.1.4 Visual Acuity and Performance

Visual acuity, often measured using an eye chart, quantifies the eye's ability to resolve fine details. It's typically expressed as a fraction (e.g., 20/20 vision), where the numerator is the test distance and the denominator is the distance at which a person with normal acuity can read the same line.

The human eye's remarkable performance in pattern recognition, depth perception, and adaptability to varying light conditions is achieved through the complex interplay of its optical components and neural processing. This sophisticated system continues to inspire developments in artificial vision systems and optical technologies.

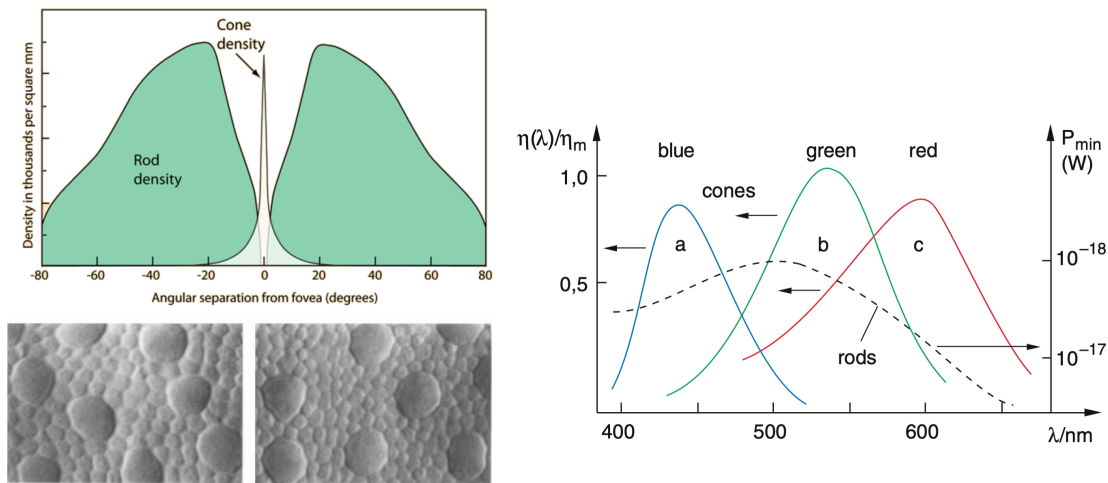


Figure 9.3: Distribution of cones and rods around the fovea, their microscopic structure, and spectral sensitivity.

9.1.5 Resolution Limit of the Eye

The resolution of the eye is limited by diffraction and the spacing of photoreceptors. The minimum angle of resolution θ_{\min} can be approximated by:

$$\theta_{\min} \approx \frac{1.22\lambda}{D}$$

where λ is the wavelength of light and D is the diameter of the pupil. For a 3 mm pupil and 555 nm light (peak sensitivity), this gives a theoretical resolution of about 1 arc minute.

9.1.6 Refractive Errors and Visual Correction

The human eye, under normal conditions, focuses images of distant objects onto the retina at the back focal distance of approximately 22 mm. However, various refractive errors can occur due to imperfections in the eye's optical system, primarily the cornea and lens. These errors affect the eye's ability to focus light accurately on the retina, leading to vision problems.

Common refractive errors include:

1. **Myopia (Short-sightedness):** Light from distant objects focuses in front of the retina, causing distant objects to appear blurry while near objects remain clear.
2. **Hyperopia (Far-sightedness):** Light focuses behind the retina, making nearby objects appear blurry while distant objects may remain clear.
3. **Astigmatism:** The cornea or lens isn't perfectly spherical, causing light to focus at multiple points rather than a single sharp point on the retina.

The severity of refractive errors can be quantified using the concept of refractive power. The refractive error R of the eye, measured in diopters (D), is calculated as:

$$R = \frac{1}{f_{\text{required}}} - \frac{1}{f_{\text{actual}}}$$

where f_{required} is the focal length needed for perfect focus, and f_{actual} is the eye's actual focal length. This formula helps determine the degree of correction needed for various eye defects.

In a normal, relaxed state, the human eye can observe objects clearly up to a distance of approximately 25 cm without additional accommodation of the lens. This distance, known as the **range of clear visual sight**,

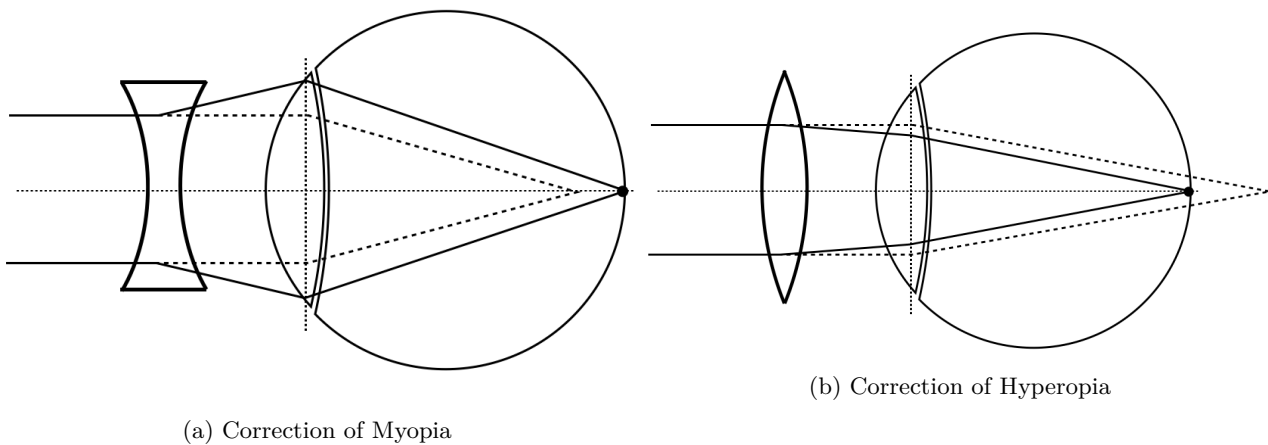


Figure 9.4: Left: Myopia correction using a concave lens. Right: Hyperopia correction using a convex lens.

varies among individuals and is used as a standard in optical calculations. Objects within this range can be observed under a visual angle θ . For small angles, which is typically the case in vision, the angular size θ of an object of height h at a distance d is approximated by:

$$\theta \approx \tan(\theta) = \frac{h}{d}$$

This relationship is fundamental in understanding how objects are perceived and in designing corrective lenses and optical instruments.

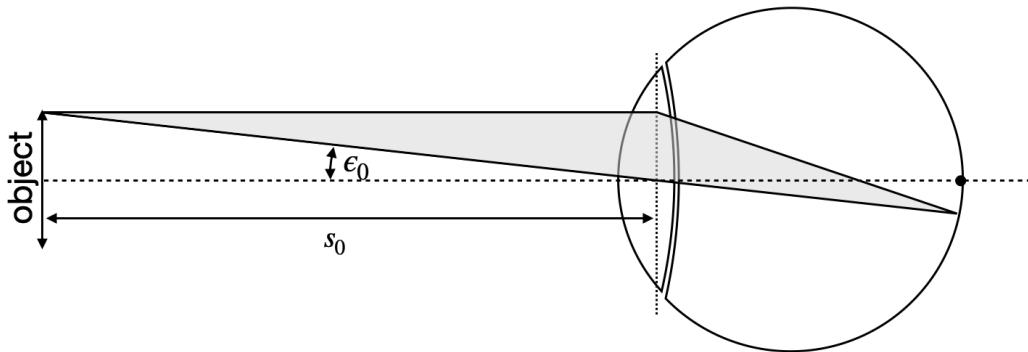


Figure 9.5: Diagram of a relaxed eye focusing on a distant object.

Understanding these concepts is crucial for diagnosing vision problems and designing appropriate corrective measures, whether through eyeglasses, contact lenses, or surgical interventions.

9.1.7 Magnification

Having discussed the basic structure and function of the human eye, we now turn to how optical instruments can enhance our vision. Instead of calculating the magnification of optical instruments from object and image distances, we introduce a more relevant measure: the **angular magnification**.

The angular magnification, V , is defined as the ratio of the angle subtended by the image when viewed through the instrument to the angle subtended by the object when viewed with the naked eye at the near point. It is given by:

$$V = \frac{\tan(\epsilon)}{\tan(\epsilon_0)} \approx \frac{\epsilon}{\epsilon_0}$$

where: - ϵ is the angle subtended by the image at the eye when viewed through the instrument - ϵ_0 is the angle subtended by the object when viewed with the naked eye at the near point

This concept is crucial in understanding how optical instruments like telescopes and microscopes enhance our vision. Angular magnification effectively increases the apparent size of objects by increasing the angle at which they are viewed. This measure is particularly useful as the actual image size is often not directly accessible or relevant to the viewer's experience.

Chapter 10

Optical Instruments

Optical instruments now combine a number of optical elements or even consist only out of a single one as in the case of the magnifying glass or the eye.

10.1 Magnifying Glass

A magnifying glass has several applications. First of all, it allows to see objects with details that would otherwise be too small to be observed with the eye even if the eye lens can accommodate to the distances. Such magnifying glasses are also used in microscopes as the so-called **eye-piece** as we will later see in the section on microscopes.

Consider the sketch below. The sketch shows an object of a size A which is at a distance of s_0 from the eye. The object makes an angle ϵ_0 with the optical axis. If we insert now a lens into the space between object and eye and the lens is positioned in a way that it is exactly at a distance f (the focal distance of the lens) from the object then we are able to observe the object under a different angle ϵ .

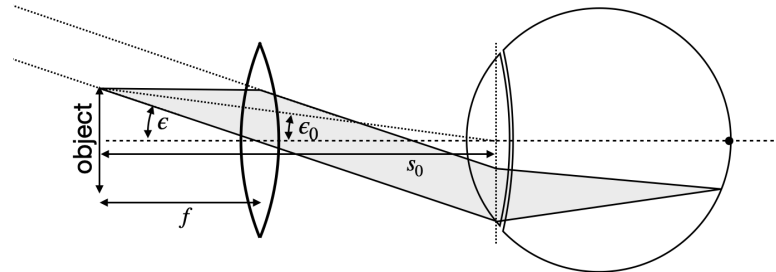


Figure 10.1: Magnifying glass at the focal distance.

The magnification of this magnifying glass can be calculated from the angles $\epsilon \approx A/f$ and $\epsilon_0 \approx A/s_0$:

$$V = \frac{\tan(\epsilon)}{\tan(\epsilon_0)} \approx \frac{\epsilon}{\epsilon_0} = \frac{A}{f} \frac{s_0}{A} = \frac{s_0}{f}.$$

The angular magnification is, thus, just given by the ratio of the clear visual range to the focal distance of the lens. If the focal distance f becomes much smaller than s_0 , large magnifications are possible.

A second very useful effect is that when the object is placed inside the focal distance from the lens, the eye images a virtual image at infinite distance to the retina (see sketch). This means the eye muscle can stay relaxed when observing the object, while it would otherwise probably have to accommodate to the distance.

Yet, placing the object at exactly the focal distance is rather tedious when holding the magnifying glass by hand. If the object is now placed inside the focal distance of the magnifying glass, we may also calculate a magnification in this case knowing the virtual image size B created in this case (see sketch below)

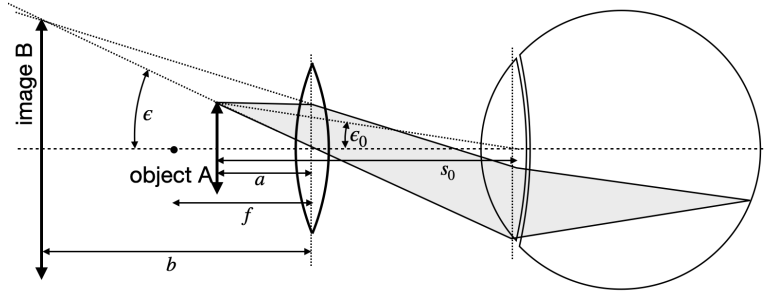


Figure 10.2: Magnifying glass for an object inside the focal range of the lens.

If a is the distance of the object from the principle plane of the magnifying glass and b and B are the distance and the size of the virtual image, respectively, we obtain

$$V = \frac{\tan(\epsilon)}{\tan(\epsilon_0)} \approx \frac{\epsilon}{\epsilon_0} = \frac{B s_0}{b A} = \frac{s_0}{a}.$$

Using the imaging equation

$$\frac{1}{f} = \frac{1}{a} + \frac{1}{b}$$

we may finally arrive at

$$V = \frac{s_0(b - f)}{b f}$$

in this case. If we place the virtual image directly at the clear visual range, i.e., $b = -s_0$, we find

$$V = \frac{s_0}{f} + 1.$$

Chapter 11

Optical Instruments

11.1 Microscope

Historical Context of Microscope Development

Optical Microscopy has a rich history of development, and is a very important tool in the fields of biology, materials science, and nanotechnology. Here are some key milestones in the history of microscopy:

Ancient Times - 13th Century: Simple magnifying glasses - The concept of magnification was known to ancient civilizations. - In the 13th century, Italian craftsmen created the first wearable glasses.

1590: Compound Microscope - Hans and Zacharias Janssen, Dutch spectacle makers, created the first compound microscope.

1665: Robert Hooke's "Micrographia" - Hooke published detailed observations made with his improved compound microscope. - He coined the term "cell" after observing cork tissue.

1670s: Antonie van Leeuwenhoek's Single-Lens Microscopes - Developed high-quality single-lens microscopes with up to 270x magnification. - First to observe and describe bacteria, yeast, and other microorganisms.

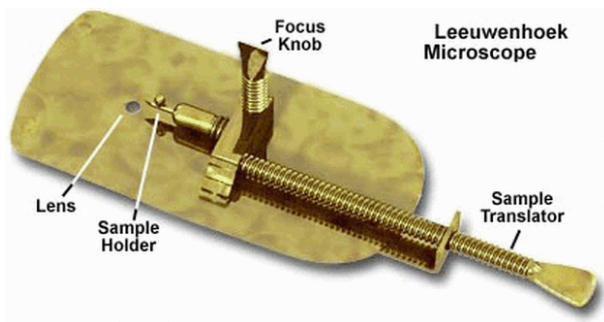


Figure 11.1: Image of Leeuwenhoek's microscope

18th-19th Centuries: Achromatic Lenses - Joseph Jackson Lister developed achromatic lenses, reducing chromatic aberration.

1830s: Ernst Abbe's Theoretical Work - Formulated the Abbe Sine Condition, crucial for modern lens design.

Late 19th Century: Oil Immersion Lenses - Allowed for higher resolution in light microscopy.

1931: Electron Microscope - Ernst Ruska and Max Knoll developed the first electron microscope.

1950s-1960s: Phase Contrast and Fluorescence Microscopy - Frits Zernike invented phase contrast microscopy. - Development of fluorescence microscopy techniques.

1981: Scanning Tunneling Microscope - Gerd Binnig and Heinrich Rohrer invented the STM, allowing

imaging at the atomic level.

1980s-Present: Digital and Computational Microscopy - Integration of CCD cameras and digital imaging. - Development of confocal microscopy, super-resolution techniques, and computational methods like ptychography.

In this section we will analyze the optical properties of microscopes from the perspective of geometrical optics which explains image formation. Yet, the key to the performance of a microscope is the understanding provided by wave optics. We will discuss this in a later section. The simplest form of a microscope consists of an objective lens with a focal distance f_1 and a magnifying glass called eye-piece with a focal length f_2 . In this system of two lenses (which are itself systems of lenses in modern microscopes, see below),



Figure 11.2: Fig.: Cut through a microscope objective lens (left) and an eye-piece.

the object is placed at a distance $a_1 < f_1 < 2f_1$ from the objective lens creating a real and reversed image at a distance b_1 behind the lens. This reversed image is observed by the eye through the eye-piece. The image of the objective lens is thereby adjusted to appear at the focal distance of the eye-piece.

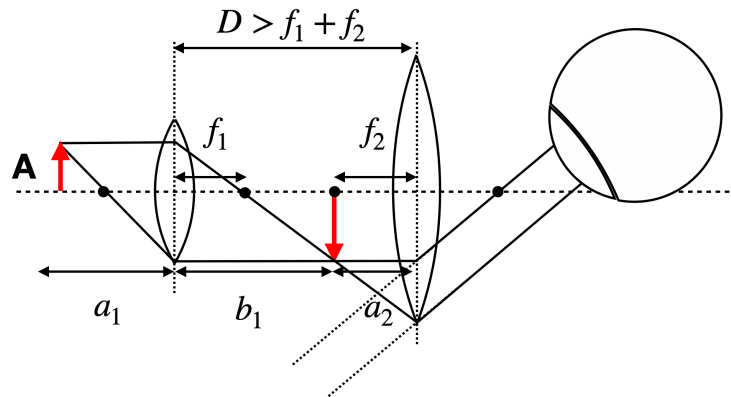


Figure 11.3: Fig.: Sketch of a simple microscope. The strange object on the right is an eye.

For this simple microscope system we may calculate first the intermediate image position b_1 :

$$\frac{1}{f_1} = \frac{1}{a_1} + \frac{1}{b_1}$$

resulting in

$$b_1 = \frac{a_1 f_1}{a_1 - f_1}.$$

If we assume a δ to be the distance of the object from the focal point of the objective lens, we even find for $\delta \rightarrow 0$

$$b_1 = \frac{a_1 f_1}{\delta}.$$

The intermediate image of size B_1 is now imaged by a magnifying glass of focal distance f_2 . According to what we calculated earlier, we have now the observation angle

$$\tan(\epsilon) = \frac{B_1}{f_2} = \frac{Ab}{a_1 f_2}.$$

If we observe the object of a size A and the clear visual distance s_0 , it would cover an angle of

$$\tan(\epsilon_0) = \frac{A}{s_0}$$

and we may obtain the total angular magnification

$$V = \frac{Ab_1 s_0}{Ab_1 f_2} = \frac{b_1 s_0}{g f_2}.$$

If we set the distance between the two lenses to $D = b_1 + f_2$ and $g \approx f_1$ then we obtain

$$V = \frac{(D - f_2)s_0}{f_1 f_2}$$

which says that the magnification is the result of the two focal length f_1, f_2 .

Modern microscopy

While the description above accurately represents the simplest microscope design, contemporary microscopes employ more intricate light paths and generally utilize what is known as **infinity corrected** optics. This system incorporates an objective lens that projects images of objects in the focal plane to infinity. Such an objective lens is invariably paired with a secondary lens, called the **tube lens**. Together, these lenses are engineered to provide a magnification level that is specified on the objective lens housing.

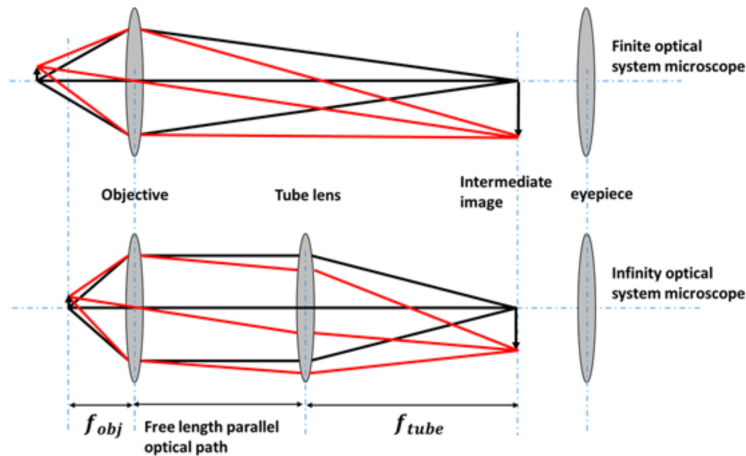


Figure 11.4: **Fig.:** Infinity optics vs. normal microscopy optics.

Infinity optics allows you to have a free length with a parallel optical path where you can insert optical elements. There is no fixed tube length as in the case sketched above, where the distance of the intermediate image has to be considered. Therefore, it has tremendous technical advantages. Common optical microscopes are further

today coupled to CCD cameras to record images digitally. Yet, an eye-piece may still be available in many cases. The sketch below shows the light path for a simple fluorescence microscope recording fluorescence images with a camera.

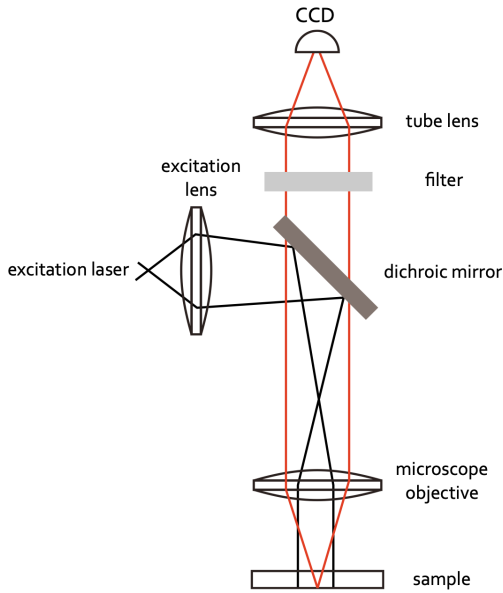
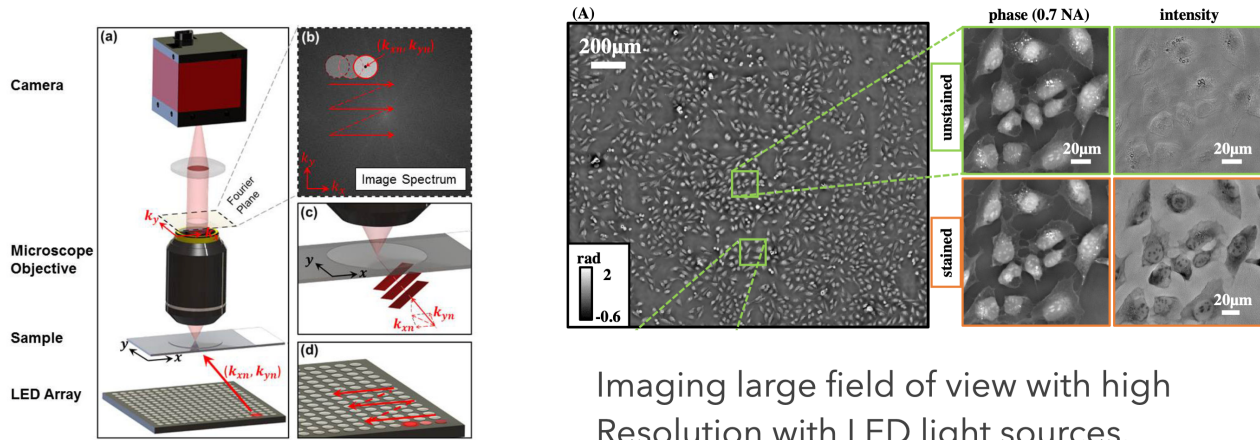


Figure 11.5: Fig.: Simple fluorescence microscope.

Digital Microscopy

The possibility to digitally record images creates endless possibilities to computationally enhance and combine images. Nowadays the field of optics is one of the fastest developing fields in physics with numerous new techniques appearing every week. In this field of imaging methods of machine learning also play an increasingly important role. While I'm not able to refer to all possible optical microscopy techniques here, I will exemplarily show some data from the Waller group at Berkley using computational methods to enhance the resolution by keeping at the same time a large field of view for imaging. This technique is called **ptychography** and can be understood if you consider Fourier Optics (a field of optics describing light propagation in terms of Fourier transforms).



Imaging large field of view with high Resolution with LED light sources.

Figure 11.6: Fig.: Ptychographic imaging with LED arrays.

There is a massive amount of other techniques with increadible images being generated. Have a look around.

i Advanced Microscopy Techniques

While traditional light microscopy has been invaluable, it's limited by the diffraction of light, restricting resolution to about 200 nm as will be discussed in a later part of this course. Modern techniques have pushed beyond this limit, revolutionizing our ability to visualize microscopic structures.

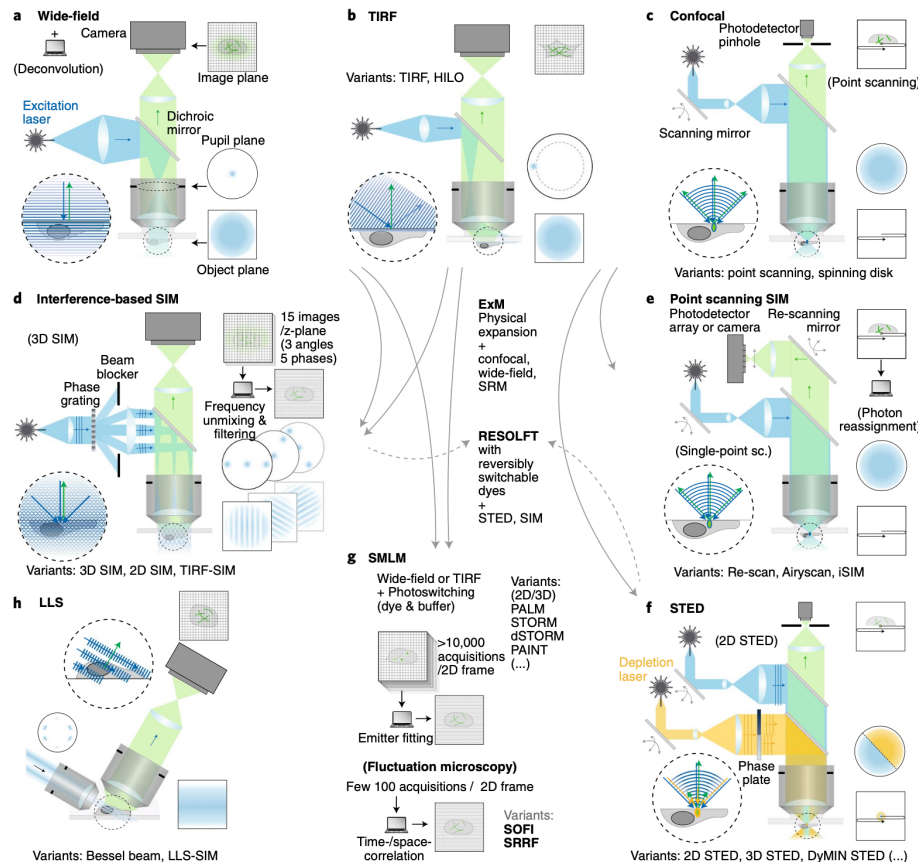


Figure 11.7: Super resolution Imaging Methods Overview (Schermelleh, L. et al. Super-resolution microscopy demystified. Nat. Cell Biol. 21, 72–84 (2019))

11.1.1 Confocal Microscopy

Confocal microscopy uses point illumination and a pinhole in an optically conjugate plane in front of the detector to eliminate out-of-focus signal.

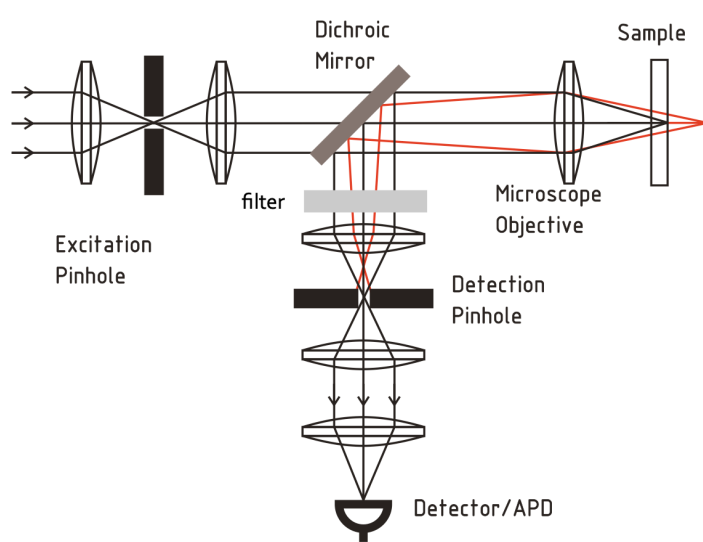


Figure 11.8: Confocal Microscope.

- **Key Features:**
 - Improved optical resolution and contrast
 - Ability to collect serial optical sections from thick specimens
 - Widely used in biological sciences
- **Overcoming Limitations:**
 - Eliminates background information away from the focal plane
 - Allows for 3D reconstruction of samples

11.1.2 Examples for Super-Resolution Microscopy Techniques

Super-resolution techniques bypass the diffraction limit, achieving resolutions down to tens of nanometers.

1. **Stimulated Emission Depletion (STED) Microscopy**
 - Uses two laser beams: one to excite fluorescent molecules, another to suppress fluorescence around the excitation spot
 - **Overcoming Limitations:** Achieves resolution as fine as 20-50 nm by precisely controlling which fluorophores are allowed to fluoresce
2. **Photoactivated Localization Microscopy (PALM)**
 - Relies on selective activation and sampling of sparse subsets of photoactivatable fluorescent molecules
 - **Overcoming Limitations:** Locates individual molecules with nanometer precision by isolating their signals over time
3. **Stochastic Optical Reconstruction Microscopy (STORM)**
 - Similar to PALM, but uses photoswitchable fluorophores
 - **Overcoming Limitations:** Achieves resolutions of ~20 nm by precisely locating the centers of single fluorescent molecules
4. **Structured Illumination Microscopy (SIM)**
 - Uses patterned illumination to create moiré fringes, which are computationally processed to reconstruct super-resolution images
 - **Overcoming Limitations:** Doubles the resolution of traditional light microscopy to ~100 nm
5. **Superresolution Photothermal Infrared Imaging**
 - Superresolution photothermal infrared imaging is a novel technique that brings the advantages of superresolution microscopy to the infrared regime.
 - **Overcoming Limitations:** Achieves resolutions of ~300 nm for infrared imaging at wavelength of 10 μm by using photothermal lensing effects.